Published October 8, 2012

Cdk1 and Plk1 mediate a CLASP2 phospho-switch that stabilizes kinetochore–microtubule attachments

Ana R.R. Maia,[1,2] Zaira Garcia,[1] Lilian Kabeche,[3,4] Marin Barisic,[1] Stefano Maffini,[1] Sandra Macedo-Ribeiro,[1] Iain M. Cheeseman,[5] Duane A. Compton,[3,4] Irina Kaverina,[2] and Helder Maiato[1,6]

[1]Instituto de Biologia Molecular e Celular, Universidade do Porto, Rua do Campo Alegre 823, 4150-180 Porto, Portugal
[2]Department of Cell and Developmental Biology, Vanderbilt University Medical Center, Nashville, TN 37232
[3]Department of Biochemistry, Dartmouth Medical School, Hanover, NH 03755
[4]Norris Cotton Cancer Center, Lebanon, NH 03766
[5]Whitehead Institute for Biomedical Research and Department of Biology, Massachusetts Institute of Technology, Cambridge, MA 02142
[6]Department of Experimental Biology, Faculdade de Medicina, Universidade do Porto, 4200-319 Porto, Portugal

Accurate chromosome segregation during mitosis relies on a dynamic kinetochore (KT)–microtubule (MT) interface that switches from a labile to a stable condition in response to correct MT attachments. This transition is essential to satisfy the spindle-assembly checkpoint (SAC) and couple MT-generated force with chromosome movements, but the underlying regulatory mechanism remains unclear. In this study, we show that during mitosis the MT- and KT-associated protein CLASP2 is progressively and distinctively phosphorylated by Cdk1 and Plk1 kinases, concomitant with the establishment of KT–MT attachments. CLASP2 S1234 was phosphorylated by Cdk1, which primed CLASP2 for association with Plk1. Plk1 recruitment to KTs was enhanced by CLASP2 phosphorylation on S1234. This was specifically required to stabilize KT–MT attachments important for chromosome alignment and to coordinate KT and non-KT MT dynamics necessary to maintain spindle bipolarity. CLASP2 C-terminal phosphorylation by Plk1 was also required for chromosome alignment and timely satisfaction of the SAC. We propose that Cdk1 and Plk1 mediate a fine CLASP2 "phospho-switch" that temporally regulates KT–MT attachment stability.

Introduction

At the onset of mitosis, microtubule (MT) dynamics increase as a result of activation and action of Cdk1 over MT-associated proteins, favoring the "search-and-capture" of chromosomes by centrosomal MTs (Kirschner and Mitchison, 1986). Upon attachment to kinetochores (KTs), MTs become gradually stabilized, forming KT-fibers (k-fibers), whereas cross-linking between non-KT–MTs with opposite polarity establish the interpolar MTs. KT–MT attachment stability must be finely regulated to allow, on one hand, the correction of erroneous MT attachments resulting from the stochastic interaction between KTs and MTs and, on the other hand, the stabilization of correct KT–MT attachments (Bakhoum and Compton, 2011; Matos and Maiato, 2011). As chromosomes bi-orient relative to spindle poles and start experiencing tension caused by opposing spindle-pulling forces, MT lifetime at KTs increases (Zhai et al., 1995; Bakhoum et al., 2009b). This labile-to-stable transition is critical in satisfying the spindle-assembly checkpoint (SAC) and allowing efficient force transduction by depolymerizing MTs to power chromosome segregation during anaphase. Importantly, just a few-fold increase in KT–MT stability during early mitosis in normal untransformed human cells is sufficient to induce chromosome segregation defects to levels comparable to those in cancer cells with chromosomal instability (CIN), whereas stimulation of KT–MT turnover is able to restore stability to otherwise chromosomally unstable tumor cells (Bakhoum et al., 2009a,b). Thus, there is a causal relationship between deregulation of KT–MT dynamics and CIN. However, surprisingly little is known about how specific KT proteins are regulated to fine tune KT–MT dynamics throughout mitosis.

Z. Garcia, L. Kabeche, and M. Barisic contributed equally to this paper.

Correspondence to Helder Maiato: maiato@ibmc.up.pt

S. Maffini's present address is the Max Planck Institute of Molecular Physiology, Dortmund, Germany.

Abbreviations used in this paper: CIN, chromosomal instability; IP, immunoprecipitate(d); KT, kinetochore; MT, microtubule; SAC, spindle-assembly checkpoint.

Supplemental Material can be found at:
http://jcb.rupress.org/content/suppl/2012/10/04/jcb.201203091.DC1.html
Original image data can be found at:
http://jcb-dataviewer.rupress.org/jcb/browse/5424

The Rockefeller University Press $30.00
J. Cell Biol. Vol. 199 No. 2 285–301
www.jcb.org/cgi/doi/10.1083/jcb.201203091

Published October 8, 2012

Polo-like kinase 1 (Plk1) has been implicated in the regulation of KT–MT attachments (Sumara et al., 2004; Peters et al., 2006; Lénárt et al., 2007) through phosphorylation of distinct KT substrates (Li et al., 2010; Bader et al., 2011; Hegemann et al., 2011; Kettenbach et al., 2011; Santamaria et al., 2011; Hood et al., 2012). In addition to the kinase domain at the N terminal, Plk1 contains a noncatalytic region at its C terminal termed the Polo-box domain (PBD), which recognizes the core consensus motif S-(pT/pS)-(P/X) on its mitotic substrates, upon priming Cdk1 phosphorylation (Cheng et al., 2003; Elia et al., 2003a,b). The PBD has been shown to be important for the recruitment of Plk1 to diverse mitotic structures, such as centrosomes, KTs, and spindle midzone/midbody (Seong et al., 2002; Elia et al., 2003a). In the particular context of KTs, Plk1 recruitment has been shown to rely on the SAC protein Bub1, PBIP1, and the cytoplasmic dynein-associated protein NudC (Kang et al., 2006; Nishino et al., 2006; Qi et al., 2006).

Human CLASP1 and CLASP2 (CLASPs) are conserved MT plus-end tracking proteins involved in the regulation of MT dynamics throughout the cell cycle. In interphase, CLASPs stabilize MT plus-ends, thereby promoting MT growth from centrosomes and the Golgi apparatus (Akhmanova et al., 2001; Efimov et al., 2007), a process that is regulated by GSK3β (Kumar et al., 2009). During mitosis, CLASPs remain associated with centrosomes, where they regulate mitotic spindle positioning and pole integrity (Samora et al., 2011; Logarinho et al., 2012). Before anaphase, independently of their association with MTs and centrosomes, CLASPs also localize to KTs, where they promote flux and turnover of attached MTs required to ensure mitotic spindle bipolarity/size, as well as proper chromosome alignment and segregation (Maiato et al., 2003a,b; Pereira et al., 2006; Maffini et al., 2009; Logarinho et al., 2012). Recently, CLASP1 was found to associate and recruit the MT depolymerase Kif2b to KTs (Manning et al., 2007, 2010), explaining how CLASPs promote MT turnover at KTs early in mitosis. Interestingly, the CLASP1 interaction with Kif2b at unattached KTs is replaced by an interaction with the MT-stabilizing protein Astrin, as MTs attach to KTs and chromosomes bi-orient (Manning et al., 2010). As such, CLASP1 was proposed to be part of a molecular switch that regulates the transition from labile-to-stable MT attachments through interaction with temporally distinct molecular partners at KTs. Upon entry into anaphase, CLASPs are recruited to the spindle midzone by PRC1, where they mediate the organization of midzone MTs, spindle elongation, and cytokinesis (Maiato et al., 2003a; Pereira et al., 2006; Liu et al., 2009). Therefore, MT regulation by CLASPs is associated with spatially and temporally distinct processes throughout mitosis, but the underlying regulatory mechanism is unknown.

In this study, we investigate the temporal regulation of CLASPs function at KTs and the respective impact on KT–MT dynamics. We found that a specific and single-priming, Cdk1-mediated phosphorylation of CLASP2, but not CLASP1, creates a docking site for Plk1 interaction and recruitment to KTs. CLASP2 is also phosphorylated by Plk1, which is enhanced by Cdk1 activity. Functional assays show that CLASP2 phosphorylation by Cdk1 and Plk1 is required for normal chromosome alignment during mitosis, but these phosphorylations distinctively affect mitotic spindle bipolarity. We propose that Cdk1 and Plk1 mediate a CLASP2 phospho-switch that is necessary to stabilize KT–MT attachments in human cells.

Results

CLASP2 is phosphorylated during mitosis at its C-terminal domain

To investigate how CLASPs function is regulated during mitosis, we started by comparing their respective mobility profiles on SDS-PAGE using protein extracts from asynchronous and mitotic-enriched HeLa cells upon Western blot analysis with specific CLASP1 and CLASP2 monoclonal antibodies (Maffini et al., 2009). Although CLASP1 presented only a slight mobility change in mitosis, CLASP2 showed a clear and distinctive band shift to a higher molecular weight, suggesting differential regulation of CLASPs during mitosis (Fig. 1 A). To dissect the nature of the observed CLASP2 band shift we immunoprecipitated (IP) the endogenous protein from asynchronous and mitotic-enriched cell populations, followed by treatment with λ-phosphatase to remove all phosphate groups. Because the CLASP2 band shift disappeared after λ-phosphatase treatment, we concluded that CLASP2 is extensively phosphorylated during mitosis (Fig. 1 B). Notably, λ-phosphatase treatment slightly increased the mobility of CLASP2, even in extracts from asynchronous cells, suggesting some level of CLASP2 phosphorylation during interphase, in agreement with previously reported regulation of CLASP2 function by GSK3β (Kumar et al., 2009). To confirm CLASP2 phosphorylation in mitosis, we released HeLa cells from a double thymidine block and followed CLASP2 mobility over time. We found a significant CLASP2 band shift that was correlated with its increased phosphorylation and high cyclin B levels (Fig. S1 A).

In an attempt to map a specific phosphorylation domain of CLASP2 responsible for the observed band shift during mitosis, we expressed several GFP-CLASP2 deletion constructs in HeLa cells, and analyzed the respective protein extracts by Western blot with anti-CLASP2 and anti-GFP antibodies (Fig. S1 B). We found that the main phosphorylation region responsible for the typical band shift of CLASP2 on SDS-PAGE is localized at its C-terminal domain, between residues 1093 and 1237 (Fig. 1 C). Given the close sequence similarity between CLASPs and the previous implication of CLASP1 C-terminal for KT localization (Maiato et al., 2003a) we performed a parallel immunofluorescence analysis to ascertain for KT recruitment of the different GFP-CLASP2 mutants (Fig. S1 C). The results are summarized in Fig. 1 C and indicate that CLASP2 is phosphorylated in vivo close to its KT-targeting domain.

CLASP2 phosphorylation during mitosis is mediated by Cdk1 and Plk1

With the aim of identifying the kinases responsible for CLASP2 phosphorylation during mitosis, we used specific small-molecule

Published October 8, 2012

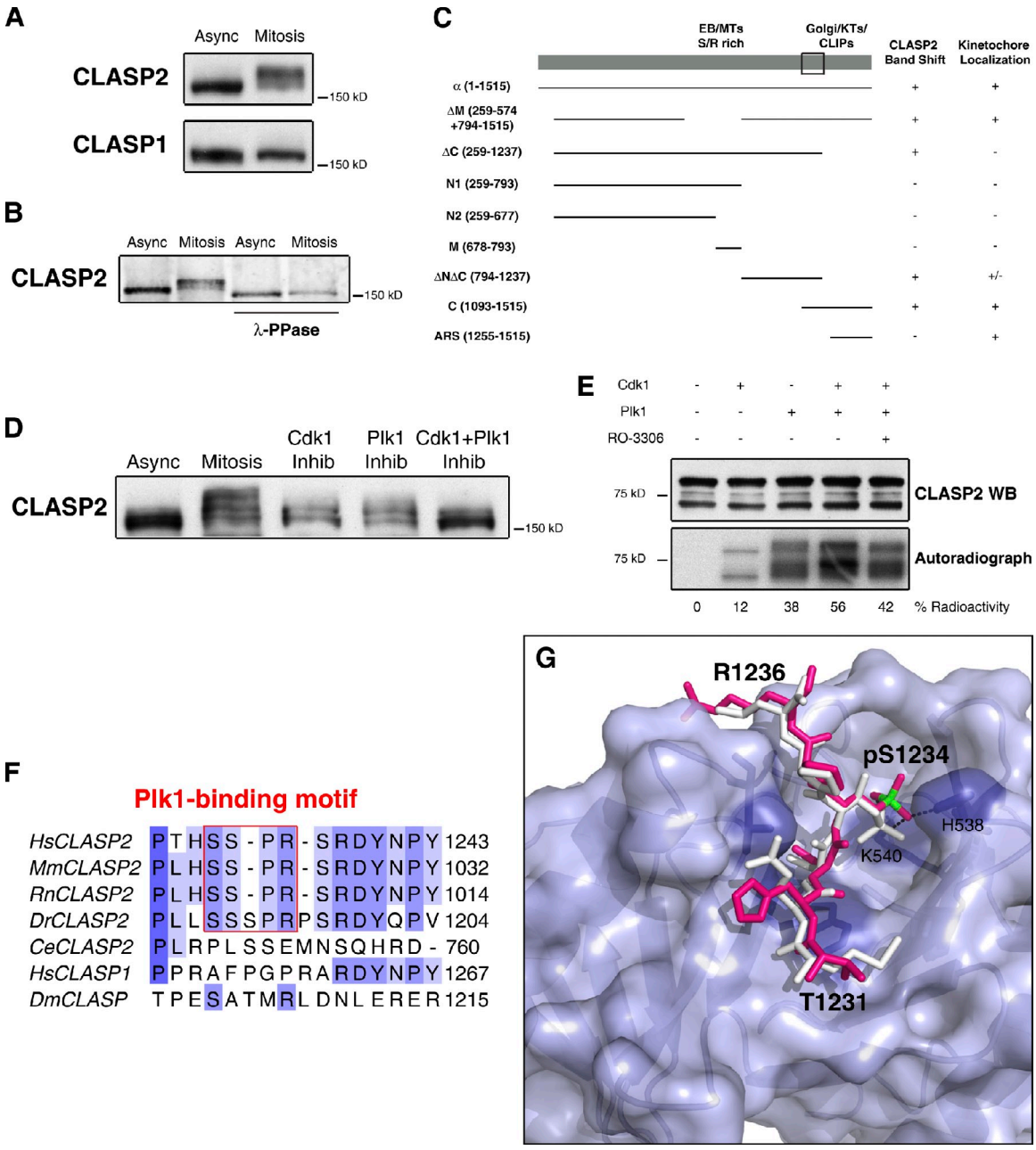

Figure 1. **The C-terminal domain of CLASP2 is phosphorylated during mitosis by Cdk1 and Plk1.** (A) Western blotting of CLASP1 and CLASP2 from asynchronous (Async) and mitotic (Mitosis) HeLa cells. (B) Western blotting of CLASP2 from asynchronous and mitotic protein extracts IP for CLASP2, before and after λ-phosphatase treatment. (C) Summary of the absence (−) or presence (+) of the mitotic band shift and respective KT localization of GFP-CLASP2 deletion mutants (amino acid region in brackets). The box represents the minimal region of CLASP2 accounting for the observed band-shift. (D) Asynchronous, mitotic, Cdk1, and/or Plk1 kinase inhibited mitotic HeLa cell protein extracts resolved by SDS-PAGE and immunoblotted for CLASP2. (E) In vitro kinase assay with recombinant CLASP2 C terminal in the presence of active Cdk1 and Plk1 kinases. Top panel shows CLASP2 Western blot, and bottom panel shows [^{32}P]ATP gel autoradiography. Kinase activity on CLASP2 was determined by the percentage of radioactive ATP incorporation. (F) Multiple sequence alignment of CLASPs in several organisms. The Plk1-binding motifs in CLASP2 are boxed in red. (G) Surface representation of Plk1 PBD. The MQSpTPL peptide (white) and the model of the 1231-THSpSPR-1236 CLASP2 fragment (magenta, with phosphorous atom highlighted in green) are shown as sticks docked at the central phosphoepitope-binding cleft on the PBD. Conserved binding cleft-forming residues interacting with the bound phosphopeptide are represented as purple sticks. The phosphoserine fits into a deep pocket and the phosphate group is stabilized by interactions with His538 and Lys540 side chains.

inhibitors of well-established mitotic kinases, including Cdk1, Plk1, Aurora B, and Mps1 (Ditchfield et al., 2003; Vassilev et al., 2006; Lénárt et al., 2007; Kwiatkowski et al., 2010). We found that only Cdk1 or Plk1 inhibition with RO-3306 and BI 2536, respectively, affected the normal mobility profile of CLASP2 during mitosis, reducing the characteristic band shift on SDS-PAGE (Figs. 1 D and Fig. S1 D). Importantly, simultaneous Cdk1 and Plk1 inhibition revealed a cumulative effect over CLASP2 mobility during mitosis (Fig. 1 D), suggesting that both Cdk1 and Plk1 phosphorylate CLASP2 at distinct sites. Curiously, as in interphase, GSK3β inhibition with lithium chloride also caused a slight reduction in CLASP2 band

Published October 8, 2012

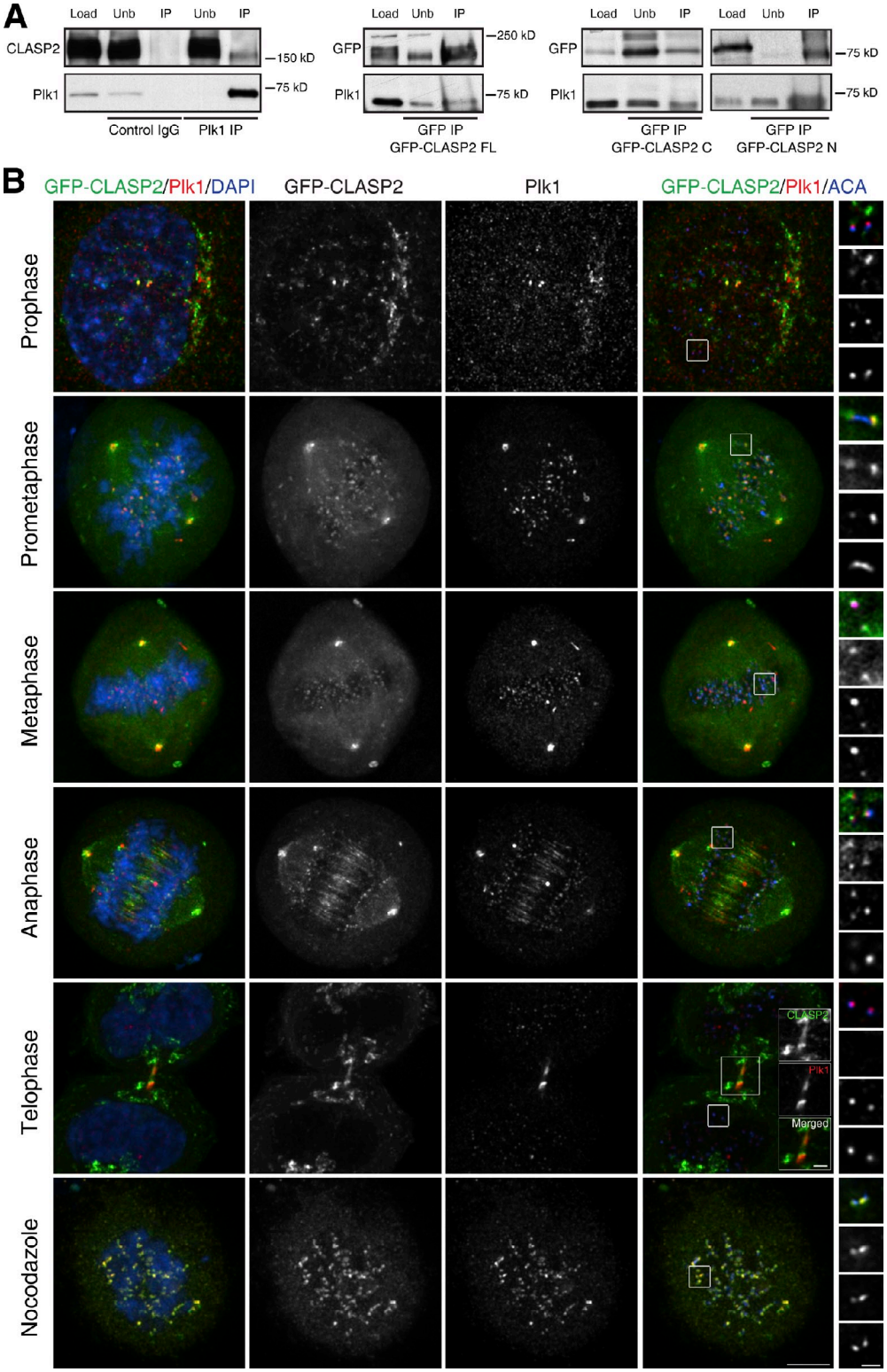

Figure 2. **CLASP2 and Plk1 interact and colocalize throughout mitosis.** (A) Western blot analysis of mitotic HeLa cell extracts IP with an unspecific IgG (Control) and Plk1 antibody (Plk1 IP). The middle and rightmost panels show GFP IPs from mitotic HeLa cells transiently expressing GFP-CLASP2 full length, C terminal, and N terminal, respectively. Total protein extracts (Load), unbound proteins (Unb), and IPs were analyzed by Western blotting with the indicated antibodies. (B) Mitotic distribution of GFP-CLASP2α (green) transiently expressed in HeLa cells and immunostained for Plk1 (red), ACA (blue, right), and DNA counterstained with DAPI (blue, left). Far right panels show KT insets of selected z planes of the respective boxed regions. From top to bottom, the images are ordered as follows: Merge, GFP-CLASP2, Plk1, and ACA. Midbody colocalization during telophase is depicted in the merged figure. Bottom panels shows a nocodazole-treated cell to highlight the MT-independent CLASP2 and Plk1 KT colocalization. Bars: 5 µm and 1 µm (higher magnifications).

Published October 8, 2012

shift during mitosis, but in a less prominent way compared with that observed upon Cdk1 and/or Plk1 inhibition (Fig. S1 E). Overall, these data implicate Cdk1 and Plk1 as major CLASP2-regulating kinases during mitosis.

To test whether Cdk1 and Plk1 directly phosphorylate CLASP2, we performed an in vitro kinase assay by adding purified and active Cdk1 and Plk1 kinases to a soluble C-terminal recombinant fragment of CLASP2 in the presence of radioactive ATP. We observed that both Cdk1 and Plk1 have the capacity to directly phosphorylate CLASP2, as determined by the incorporation of [^{32}P]ATP (Fig. 1 E). Moreover, combination of both kinases increased the total amount of [^{32}P]ATP incorporated, which could be reverted upon inhibition of Cdk1 in the reaction mix with RO-3306.

Next, we used mass spectrometry to map which residues on the CLASP2 C terminal were independently phosphorylated by Cdk1 or Plk1 in vitro. We identified three serine residues that were exclusively phosphorylated by Cdk1 (S1233, S1234, and S1250), and another four that were phosphorylated by Plk1 only (S1248, S1255, S1274, and S1313; Tables S1 and S2). Many of these phosphorylated residues on CLASP2 are conserved in vertebrates (Fig. 1 F and Fig. S1 F) and were independently confirmed in vivo in large-scale proteomic studies in human cells (Table S1 and Table S2). These residues are not conserved in human CLASP1 or on known *Xenopus tropicalis, Caenorhabditis elegans*, or *Drosophila melanogaster* CLASP orthologues (Fig. 1 F and Fig. S1 F). Overall, these experiments demonstrate that the CLASP2 C terminal is directly phosphorylated during mitosis by Cdk1 and Plk1 kinases at distinct sites. Moreover, they support the belief that the observed phosphorylations are specific to vertebrate CLASP2, providing the first molecular signatures that distinguish the two human CLASP paralogues.

CLASP2 colocalizes and interacts with Plk1 during mitosis

In-depth sequence analysis of the phosphorylated residues on the CLASP2 C terminal revealed that phosphorylation of S1234 by Cdk1 defines a putative Plk1-binding motif in vertebrates (Fig. 1 F; Elia et al., 2003a). Modeling of the 1231-THSpSPR-1236 CLASP2 fragment with the known structure of the PBD of Plk1 bound to a specific polypeptide revealed a good fit at the central phosphoepitope-binding cleft shaped by key amino acid residues from the PBD, which are known to stabilize the interactions with the phosphate group (Cheng et al., 2003; Elia et al., 2003b; Śledź et al., 2011; Fig. 1 G). Thus, phosphorylation of CLASP2 on S1234 by Cdk1 may be part of a recognition site that promotes the interaction with Plk1 during mitosis.

To determine whether CLASP2 interacts with Plk1 in vivo, we IP Plk1 from mitotic-enriched HeLa cell extracts treated with the kinesin-5 inhibitor STLC and identified endogenous CLASP2 as a co-immunoprecipitating protein (Fig. 2 A). Similarly, immunoprecipitation of full-length or C-terminal GFP-CLASP2 co-IP endogenous Plk1, demonstrating that the C-terminal domain of CLASP2 is sufficient to mediate the interaction with Plk1. Interestingly, the GFP-CLASP2 N terminal was also able to co-immunoprecipitate Plk1 (Fig. 2 A), suggesting that CLASP2 and Plk1 interact through multiple interfaces. Additionally, we observed that CLASP2 and Plk1 colocalize at KTs and centrosomes throughout mitosis, as well as at the Golgi apparatus during mitotic entry and exit (Fig. 2 B). Importantly, the KT colocalization of CLASP2 and Plk1 did not depend on MTs, as it was also verified in cells treated with micromolar doses of nocodazole. In anaphase and telophase, CLASP2 and Plk1 colocalized at spindle midzone and midbody, respectively (Fig. 2 B). These data suggest that CLASP2 and Plk1 interact at multiple structures of the mitotic apparatus.

To understand the functional significance of the observed interactions between CLASP2 and Plk1, we ectopically targeted CLASP2 to the mitochondrial outer membrane by means of a fusion with dTOM20 protein (Efimov et al., 2007). We found that CLASP2 displacement to the mitochondria promoted Plk1 recruitment to this organelle (Fig. 3 A), supporting the argument that these proteins are part of a common complex in vivo and indicating that CLASP2 is able to drive Plk1 cellular localization.

CLASP2 phosphorylation on S1234 by Cdk1 enhances Plk1 recruitment to KTs

Next, we investigated whether CLASP2 and the specific phosphorylation of S1234 were required for normal Plk1 recruitment to KTs. We started by depleting endogenous CLASP2 by RNAi (Fig. S2 A) and found that Plk1 levels at KTs were reduced by ∼50% relative to controls (Fig. 3, B and C). Consistently, CENP-E depletion by RNAi (Fig. S2 B), which specifically prevents normal CLASP2 recruitment to KTs (Maffini et al., 2009), led to a comparable and specific reduction of Plk1 levels at KTs (Fig. 3, D and E). Remarkably, overexpression of a nonphosphorylatable GFP-CLASP2 mutant (S1234A), when compared with overexpression of GFP-CLASP2 wild-type, led to a significant reduction of Plk1 levels at KTs (38%) even in the presence of endogenous CLASP2, suggesting a dominant-negative effect. Moreover, the observed reduction of Plk1 levels at KTs was proportional to that observed upon Cdk1 inhibition (43%; Fig. 3, F–H). Overexpression of a phospho-mimetic GFP-CLASP2 mutant (S1234D) significantly rescued Plk1 levels at KTs (Fig. 3 G). Note that to normalize Plk1 levels at KTs all quantifications were performed in the absence of MTs upon nocodazole treatment. Finally, we investigated whether CLASP2 phosphorylation on S1234 was important for CLASP2-Plk1 interaction by means of coimmunoprecipitation experiments with GFP-CLASP2 wild-type or GFP-CLASP2 S1234A mutant. We found that the amount of Plk1 co-immunoprecipitating with the GFP-CLASP2 S1234A mutant was reproducibly reduced ∼40% relative to the wild-type protein (Fig. 3 I). Importantly, these experiments further indicated that CLASP2–Plk1 interaction is enhanced in mitotic cells that were allowed to establish KT–MT attachments (Fig. 3 I). Overall, these data support a model in which phosphorylation of CLASP2 on S1234 by Cdk1 is required for normal Plk1 interaction and recruitment to KTs, concomitant with the establishment of MT attachments.

Published October 8, 2012

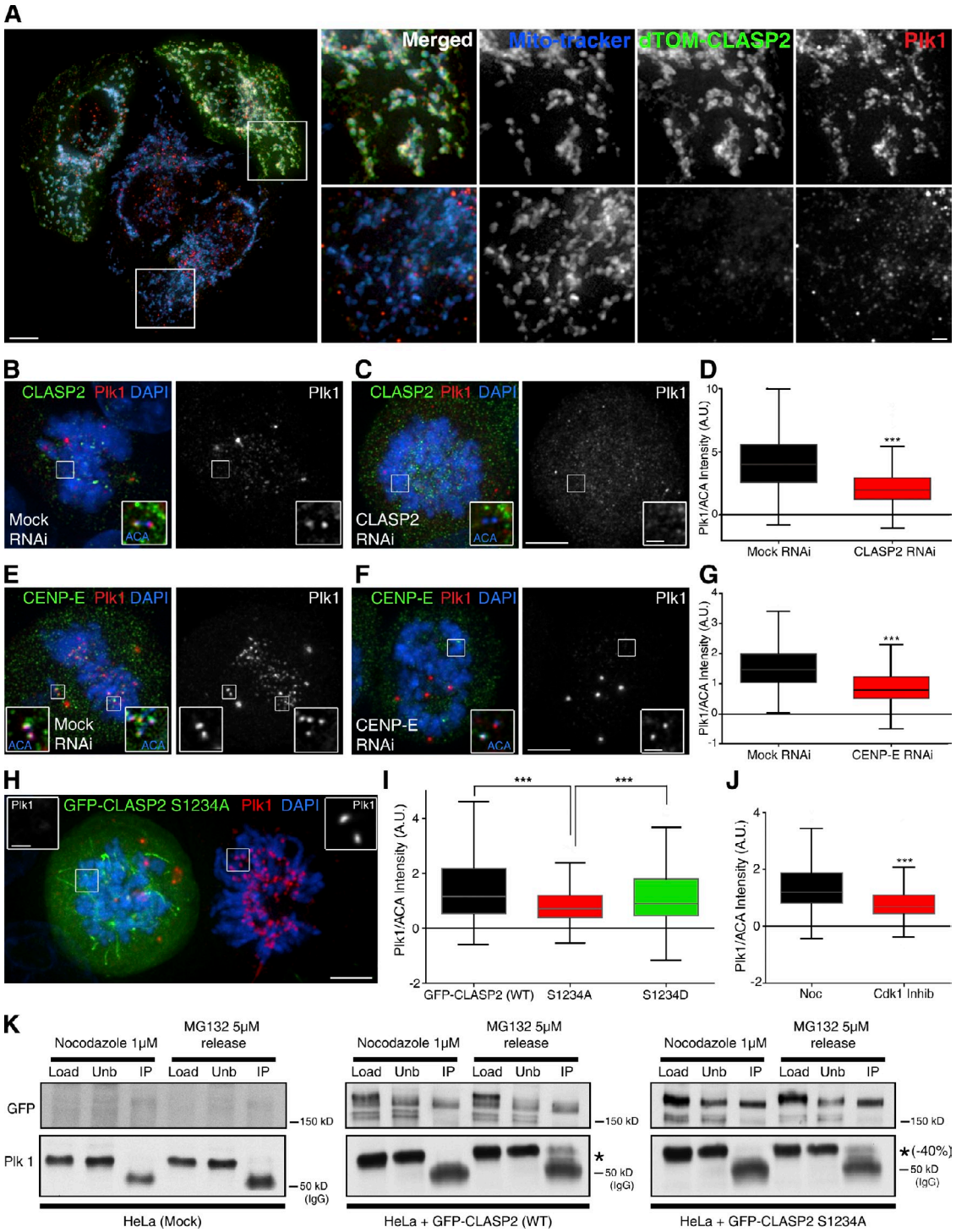

Figure 3. **CLASP2 and its phosphorylation on S1234 by Cdk1 are required for normal recruitment of Plk1 to KTs.** (A) HeLa cells transfected with dTOM20-CLASP2 construct to drive the ectopic localization of CLASP2 to the mitochondria. Cells were immunostained for Plk1 and mitochondria counter-stained with MitoTracker. (right) Insets of transfected (top) and nontransfected (bottom) cells. (B and C) Plk1 localization at KTs is reduced in HeLa cells after CLASP2 RNAi. (left) Merge image of cells immunostained for CLASP2 (green) and Plk1 (red), with DNA counterstained with DAPI (blue); (right) Plk1 localization alone. (D) Interquartile representation of normalized Plk1 KT intensity in Mock RNAi (n = 494) and CLASP2 RNAi (n = 559). Medians are statistically different, $P < 0.0001$, Mann-Whitney t test. (E and F) Plk1 localization at KTs is reduced in HeLa cells after CENP-E RNAi. (left) Merge image of cells immunostained for CLASP2 (green) and Plk1 (red), with DNA counterstained with DAPI (blue); right panel shows Plk1 localization alone. (G) Interquartile representation of normalized KT Plk1 levels, Mock RNAi (n = 483), and CENP-E RNAi (n = 492). Medians are statistically different, $P < 0.0001$, Mann-Whitney t test. (H) Overexpressing GFP-CLASP2 S1234A (green) HeLa cell (left) with an untransfected neighbor cell (right) immunostained for Plk1 (red or white in the insets) and DNA counterstained with DAPI (blues). Bars: 5 μm and 1 μm (higher magnifications). (I) Interquartile representation of normalized Plk1 intensities at KTs in cells expressing GFP-CLASP2 wild-type (n = 475), S1234A (n = 493), and S1234D mutant (n = 444). ***, medians are statistically different, $P < 0.0001$, Mann-Whitney t test. (J) Interquartile representation of normalized Plk1 KT intensities in control HeLa cells (n = 491) or upon Cdk1 inhibition (n = 459). Medians are statistically different, $P < 0.0001$, Mann-Whitney t test. All quantifications were standardized by nocodazole treatment. (K) Western blot analysis of nocodazole or nocodazole-released into MG132 HeLa cells after mock, GFP-CLASP2 WT, or S1234 transfection and IP with

Published October 8, 2012

Priming Cdk1-mediated phosphorylation of CLASP2 enhances its phosphorylation by Plk1

To determine whether Plk1-mediated phosphorylation of CLASP2 requires a priming phosphorylation by Cdk1, we developed a polyclonal antibody against phosphorylated CLASP2 on S1255, one of the residues identified to be phosphorylated by Plk1 in vitro and in vivo (Table S2). To validate the specificity of this antibody, we performed CLASP2 RNAi in HeLa cells, followed by Western blot analysis with asynchronous and mitotic-enriched protein extracts. We found that this antibody recognizes mitotic-specific bands between 165 and 200 kD, corresponding to endogenous CLASP2 and respective phosphorylated forms, which decrease after CLASP2 RNAi (Fig. S2 C). To visualize where and when phosphorylation of CLASP2 on S1255 occurs during mitosis, we performed quantitative immunofluorescence in HeLa cells using antibodies against endogenous CLASP2 and its respective phosphorylated form at S1255. We found that CLASP2 phosphorylation on S1255 was essentially confined to centrosomes and KTs from prophase to anaphase, a localization that was sensitive to CLASP2 RNAi (Figs. 4 A, Fig. S2 D, and Fig. S2 E). Fluorescence quantification of pS1255 levels at KTs relative to constitutive centromere antigens revealed that phosphorylation of CLASP2 on S1255 remains unaltered from prophase until anaphase and decreases sharply during telophase (Fig. S2 F). However, when the levels of pS1255 were normalized relative to total CLASP2 at KTs, we found an almost exclusively phosphorylated pool of CLASP2 at S1255 during prophase, which decreases sharply in prometaphase. This phosphorylated pool is then maintained during metaphase and anaphase, disappearing during telophase (Fig. S2 G). Surprisingly, the anti-pS1255 antibody also decorated the nuclear envelope during prophase, a localization that does not normally show up using antibodies against total CLASP2, but was sensitive to CLASP2 RNAi (Figs. 4 A and Fig. S2 H). However, CLASP2 phosphorylation on S1255 observed at the midbody region and centrosomes during telophase and cytokinesis was less sensitive to CLASP2 RNAi (Figs. 4 A, Fig. S2 E, and unpublished data), which reflects either unspecific labeling of the phospho-antibody or a stable phosphorylated CLASP2 pool.

To investigate whether Cdk1 regulates the phosphorylation of CLASP2 on S1255 by Plk1 at KTs, we performed quantitative immunofluorescence of nocodazole-treated cells with the anti-pS1255 antibody upon individual or combined inhibition of Cdk1 and Plk1. We found that Cdk1 inhibition alone caused a significant reduction (~50%) of CLASP2 phosphorylation on S1255 at KTs (Fig. 4, B and C). As expected, the phosphoepitope recognized by the anti-pS1255 antibody almost disappeared at KTs (90% reduction) upon Plk1 inhibition alone, an effect that was aggravated (97% reduction) in combination with Cdk1 inhibition (Fig. 4, B and C). Importantly, endogenous CLASP2 levels were unchanged upon Plk1 inhibition (unpublished data). Western blot analyses of CLASP2 phosphorylation on S1255 upon Cdk1 and/or Plk1 inhibition further corroborate our quantitative immunofluorescence results. In parallel, we developed another polyclonal antibody against phosphorylated CLASP2 on S1234, which confirmed the specific mitotic phosphorylation of CLASP2 by Cdk1 (Fig. 4 D). This phospho-epitope was found diffused in the cytoplasm of mitotic cells and was partially sensitive to CLASP2 RNAi (Fig. S2 C and not depicted). Finally, to investigate whether mitotic phosphorylation of S1234 by Cdk1 impacts overall CLASP2 phosphorylation, we compared the respective mobility of GFP-CLASP2 (wild-type) with that of GFP-CLASP2 S1234A mutant on SDS-PAGE, upon transient transfection into HeLa cells. We found that although the wild-type protein showed a significant band-shift to a higher molecular weight in mitotic cells, this was barely detectable in the nonphosphorylatable mutant (Fig. 4 E). Overall, these data support that the in vivo phosphorylation of CLASP2 on S1255 at KTs is directly mediated by Plk1 and is enhanced by Cdk1 kinase activity. In agreement, priming phosphorylation of CLASP2 by Cdk1 on S1234 appears to be critical for its overall phosphorylated status during mitosis.

CLASP2 phosphorylation on S1234 is required to maintain mitotic spindle bipolarity

To distinguish between the functional implications of CLASP2 phosphorylation on S1234 by Cdk1 and Plk1-mediated phosphorylations on the CLASP2 C terminal, we compared single or multiple nonphosphorylatable and putative phosphomimetic mutants of CLASP2 fused with GFP. Localization of all mutants during mitosis was identical to the wild-type protein (Fig. S3 and Fig. S4). Overexpression (approximately seven times that of endogenous protein levels) of the S1234A mutant in HeLa cells caused a dramatic increase in monopolar spindles with abnormally long non-KT–MTs and chromosomes organized around centrosomes (Fig. 5 A, A' and B). Equivalent overexpression of the S1234D mutant or the wild-type protein gave rise mostly to bipolar spindles (Fig. 5 B). Overexpression of the nonphosphorylatable GFP-CLASP2 mutant in all identified Plk1 phosphorylation sites at the C terminal caused a slight, but not statistically significant, increase in the formation of monopolar spindles when compared with overexpression of wild-type or respective phospho-mimetic mutant, regardless of the presence of endogenous CLASP2 (Fig. 5 B; see also Fig. 7, A and D).

To understand how the phosphorylation of CLASP2 on S1234 ensures spindle bipolarity, we overexpressed the GFP-CLASP2 S1234A mutant in HeLa mCherry-H2B-Histone cells and followed mitotic progression by spinning disk confocal microscopy. We found that spindles start off bipolar, with several misaligned chromosomes and, over time, centrosomes get closer to each other due to spindle collapse, resulting in monopolar

a GFP antibody. Native protein extracts (Load), unbound proteins (Unb), and IPs were analyzed by Western blotting with GFP or Plk1 antibodies. Asterisk indicates Plk1 and the respective reduction percentage in the S1234 mutant. The band at 50 kD corresponds to the antibody heavy chain (IgG).

Published October 8, 2012

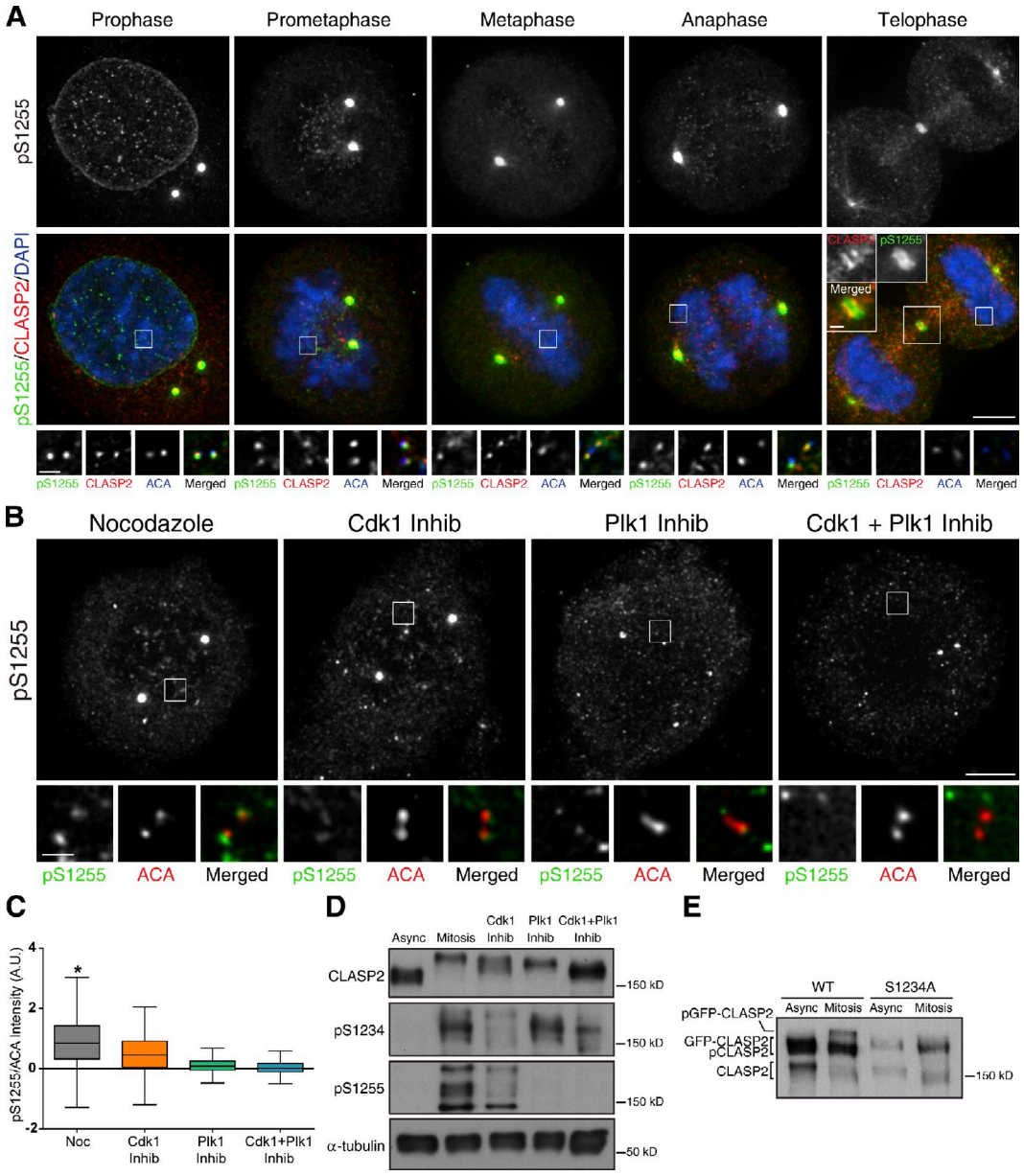

Figure 4. **CLASP2 phosphorylation by Plk1 at KTs requires Cdk1-mediated priming.** (A) Immunofluorescence localization of pS1255 epitope (green) in mitotic HeLa cells stained for total CLASP2 (red) and DNA counterstained with DAPI (blue). (top) pS1255 staining alone during mitosis. (left to right) KT insets of selected planes from z stacks of the boxed area represent pS1255, CLASP2, ACA, and Merged. Midbody colocalization during telophase is highlighted in the merged figure. (B) Representative immunofluorescence images of pS1255 at KTs upon nocodazole treatment, or combined with Cdk1, Plk1, or both kinase inhibitors. (left to right) Insets show KT single planes of the boxed regions of pS1255 (green) and ACA (red) staining. Bars: 5 µm and 1 µm (higher magnifications). (C) Interquartile representation of pS1255 KT intensities in cells treated with nocodazole (n = 491), nocodazole + Cdk1 inhibitor (n = 459), nocodazole + Plk1 inhibitor (n = 471), and nocodazole + Cdk1 + Plk1 Inhibitors (n = 429). Statistically different values are indicated with *, $P < 0.05$, Dunn's Multiple comparison test. (D) CLASP2, pS1234, pS1255, and α-tubulin Western blot of asynchronous and mitotic cells with and without inhibition of Cdk1, Plk1, or both. (E) CLASP2 Western blot analysis of asynchronous and mitotic HeLa cells expressing GFP-CLASP2 (wild-type) or GFP-CLASP2 S1234A.

spindles with abnormally long non-KT–MT bundles (Fig. 5, C and C′; and Video 1). In addition to spindle collapse, we observed that prevention of S1234 phosphorylation by Cdk1 resulted in severe chromosome alignment defects and a mitotic delay of up to several hours, ultimately resulting in cell death (Fig. 5, D and D′; and Video 2). Overall, these results support the idea that phosphorylation of CLASP2 on S1234 by Cdk1, but not phosphorylation of the CLASP2 C terminal by Plk1, is required to maintain mitotic spindle bipolarity.

CLASP2 C-terminal phosphorylation by Cdk1 and Plk1 regulates proper chromosome alignment and segregation

A smaller fraction of cells (~20%) remained bipolar upon overexpression of GFP-CLASP2 S1234A mutant (Fig. 5 B). This was likely caused by a milder overexpression, which allowed us to more directly investigate the relevance of CLASP2 phosphorylation on S1234 for chromosome alignment and mitotic progression by comparing HeLa mCherry-H2B-Histone cells

Published October 8, 2012

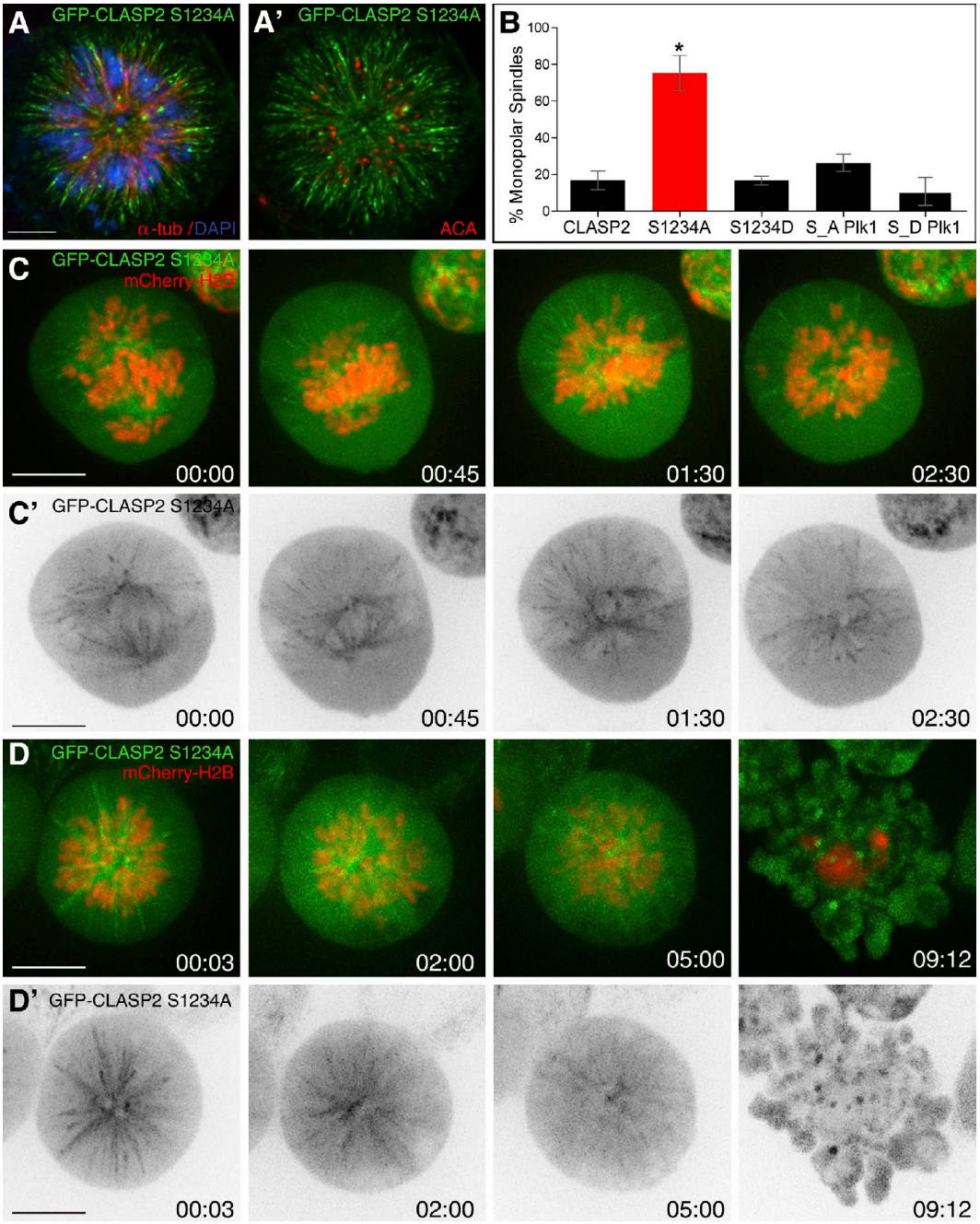

Figure 5. **CLASP2 phosphorylation on S1234 is required to maintain mitotic spindle bipolarity.** (A and A′) HeLa cell overexpressing GFP-CLASP2 S1234A mutant (green) with a monopolar spindle, immunostained for α-tubulin (red, left), ACA (red, right), and DNA counterstained with DAPI (blue, left). Bar, 5 µm. (B) Quantification of the mean percentage of monopolar spindles in cells overexpressing GFP-CLASP2 wild-type (n = 232), S1234A (n = 341), S1234D (n = 220), S_A Plk1 (n = 215), and S_D Plk1 (n = 220) from three independent experiments. Error bars refer to standard error. One-way ANOVA Bonferroni's test revealed statistically significant differences indicated with * ($P < 0.05$). (C) Mitotic spindle collapse of HeLa cells stably expressing mCherry-H2B Histone and transfected with S1234A mutant. GFP-CLASP2 S1234A or wild-type are represented in grayscale in C′. (D) Cell death in HeLa cells arrested in a monopolar conformation upon overexpression of the GFP-CLASP2 S1234A (grayscale in D′). Time is shown in hours:minutes. Bars, 10 µm.

overexpressing either GFP-CLASP2 wild-type (Fig. 6, A and A′; and Video 3) or the GFP-CLASP2 S1234A mutant (Fig. 6, B and B′; and Video 4). We found that most cells overexpressing GFP-CLASP2 wild-type progress normally throughout mitosis, but in 25% of the cases they entered anaphase in the presence of one or two misaligned chromosomes (Fig. 6 C). In contrast, >40% of the cells overexpressing the GFP-CLASP2 S1234A mutant delayed anaphase onset up to several hours, and eventually exited in the presence of misaligned chromosomes (Fig. 6, B and C). One important difference between cells overexpressing GFP-CLASP2 wild-type and S1234A mutant was the frequent (15%) presence of more than two misaligned chromosomes at anaphase onset in the latter, which led to the formation of micronuclei upon chromosome decondensation, as well as formation of chromatin bridges associated with cytokinesis failure (Fig. 6 B). Likewise, expression of the

Published October 8, 2012

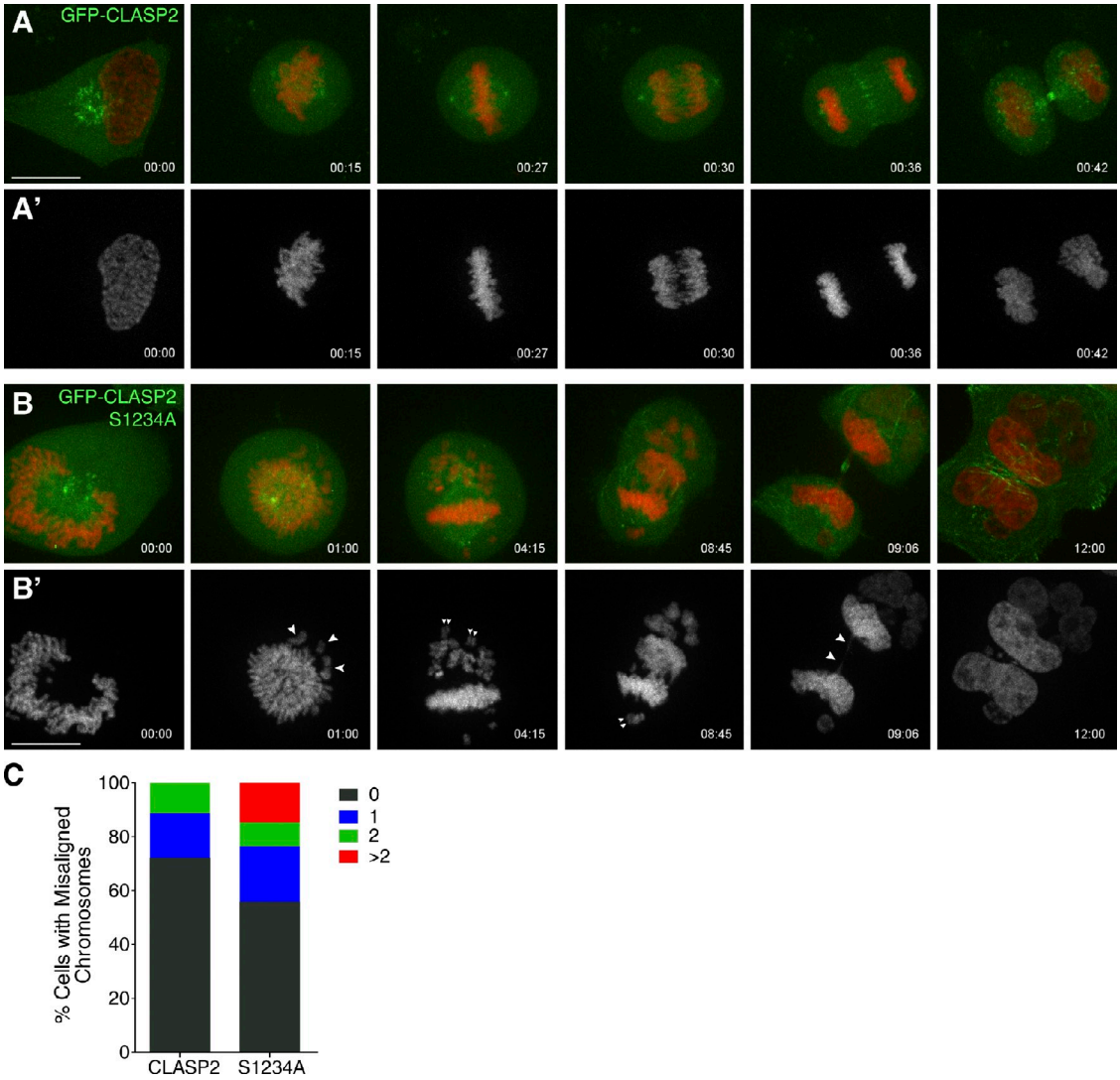

Figure 6. **CLASP2 phosphorylation on S1234 is required for normal chromosome alignment and segregation.** (A and B) Selected frames of videos from HeLa cells stably expressing mCherry-H2B Histone (red) and transiently transfected with GFP-CLASP2 wild type (green; A) or GFP-CLASP2 S1234A mutant (green; B). Images show representative frames of the videos to draw attention to chromosome alignment, segregation, and cytokinesis. A′ and B′ panels show H2B channel alone. Large arrowheads indicate misaligned and lagging chromosomes. Small arrowheads indicate sister chromatid pairs. Time is shown in hours:minutes. Bar, 10 µm. (C) Quantification of chromosome alignment defects in cells expressing GFP-CLASP2 wild-type (n = 18) or S1234A mutant (n = 34). Bars represent the percentage of cells with 0, 1, 2, or more misaligned chromosomes at anaphase onset. The results represent a pool from at least three independent experiments.

nonphosphorylatable, RNAi-insensitive GFP-CLASP2 mutant in all Plk1 phosphorylation sites at the C terminal upon depletion of endogenous CLASP2 caused a significant delay in chromosome alignment and anaphase onset (Fig. 7, A–D; and Video 5). These data support that CLASP2 phosphorylation on S1234A by Cdk1 and, more generally, at the C terminal by Plk1 are required for proper KT–MT attachments, which are important for normal chromosome alignment and timely satisfaction of the SAC.

CLASP2 phosphorylation on S1234 is specifically required to stabilize KT-MT attachments

Our previous observations indicate that phosphorylation of CLASP2 on S1234 by Cdk1 is required to maintain spindle bipolarity, chromosome alignment, and SAC satisfaction, suggesting a role in the regulation of KT–MT stability. To directly test whether phosphorylation of CLASP2 on S1234 is associated with changes in spindle MT dynamics, we photoactivated GFP-α-tubulin stably expressed in U2OS cells and determined the respective fluorescence dissipation rate over time upon transfection and overexpression of mRFP-CLASP2 wild-type or S1234A mutant, relative to untransfected controls (Fig. 8, A and B). Typically in these experiments, normalized fluorescence intensity plots are best fit by double exponential equations, in which the fast-decay component is interpreted to represent non-KT–MTs, whereas the slower-decay component likely corresponds to the more stable KT–MTs (Zhai et al., 1995; Bakhoum et al., 2009b; Maffini et al., 2009). Accordingly, we observed that overexpression of both mRFP-CLASP2

Published October 8, 2012

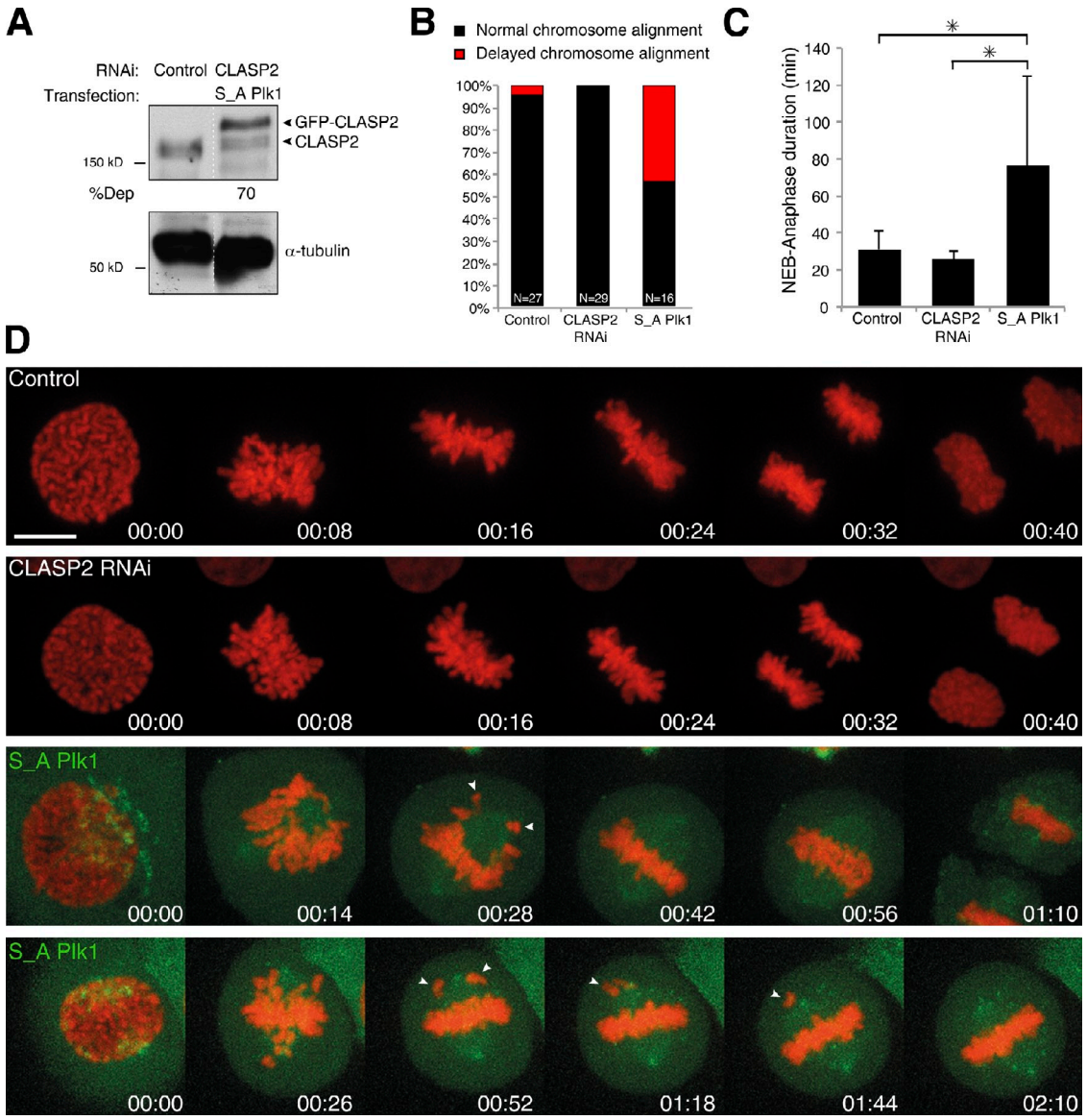

Figure 7. **CLASP2 C-terminal phosphorylation by Plk1 is required for normal chromosome alignment and mitotic duration.** (A) CLASP2 Western blot of control and endogenous CLASP2-depleted HeLa cells expressing GFP-CLASP2 S_A Plk1 mutant. (B) Quantification of HeLa mCherry-H2B Histone cells with delay in chromosome alignment in control (n = 27), CLASP2-depleted cells (n = 29), and cells depleted of CLASP2 expressing GFP-CLASP2 S_A Plk1 mutant (n = 16). The results represent a pool from at least three independent experiments. (C) Quantification of mean NEB-anaphase duration in HeLa mCherry-H2B Histone control (n = 27), CLASP2-depleted (n = 29), and cells depleted of CLASP2 expressing GFP-CLASP2 S_A Plk1 mutant (n = 16). Error bars represent standard deviations from at least three independent experiments; *, $P < 0.05$, Student t test. (D) Selected frames of representative videos of HeLa mCherry-H2B Histone (red) cells in control, CLASP2-depleted with, and CLASP2-depleted without GFP-CLASP2 S_A Plk1 mutant expression (green). Arrowheads indicate chromosomes with delayed alignment. Time is shown in hours:minutes. Bar, 10 µm.

wild-type and S1234A mutant had a similar impact on non-KT–MT turnover, leading to a significant hyperstabilization of non-KT–MTs relative to untransfected controls (Fig. 8 C, top graph). However, although overexpression of mRFP-CLASP2 wild-type also resulted in the hyperstabilization of KT–MTs, overexpression of mRFP-CLASP2 S1234A was comparable to untransfected controls (Fig. 8 C, bottom graph; note that due to a lethal combination of RNAi and overexpression of GFP-CLASP2 S1234A mutant, endogenous CLASP2 is still present in all experimental conditions). These data indicate that phosphorylation of CLASP2 on S1234 specifically stabilizes KT–MT attachments.

To test whether the observed spindle collapse upon overexpression of the CLASP2 S1234A mutant was caused by unbalanced KT versus non-KT–MT stability, as suggested by our MT-turnover measurements, we compared monopolar spindles resulting from Eg5 inhibition in cells overexpressing GFP-CLASP2 wild-type, with monopolar spindles resulting from overexpression of GFP-CLASP2 S1234A upon immunostaining for different MT markers. Namely, we detected acetylated tubulin, HURP, and PRC1, which preferentially label stable MTs (Piperno et al., 1987), KT–MTs (Silljé et al., 2006), and non-KT–MTs (Mollinari et al., 2002). In agreement with our live cell observations, we found abnormally long, calcium-stable,

Published October 8, 2012

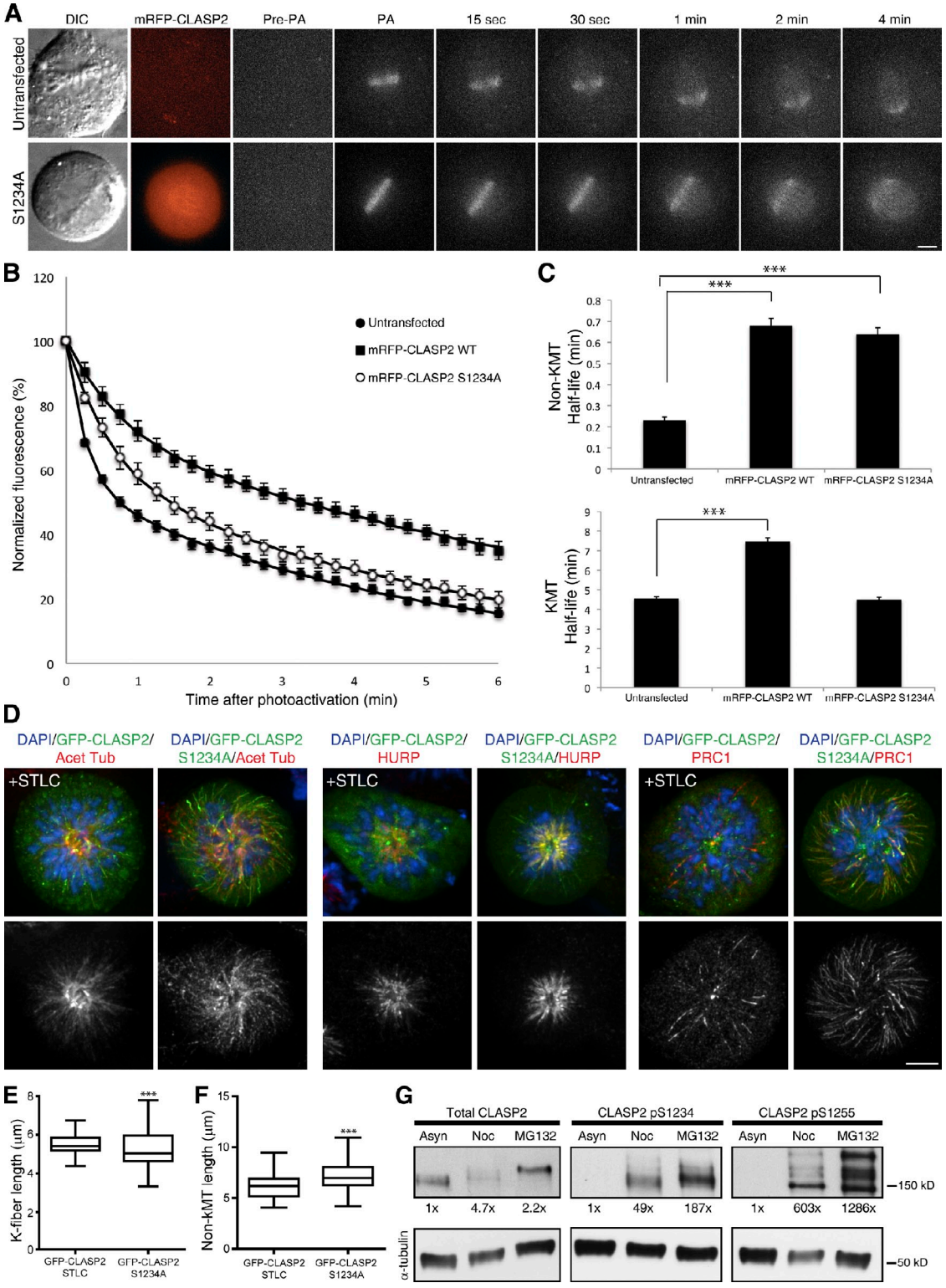

Figure 8. **Phosphorylation of CLASP2 on S1234 by Cdk1 promotes KT–MT stabilization.** (A) Time-lapse DIC and fluorescent images of metaphase spindles in untreated (control) and mRFP-CLASP2 S1234A expressing U2OS cells before photoactivation (Pre-PA) and at indicated times after photoactivation (PA) of GFP-α-tubulin. (B) Normalized fluorescence intensity over time after photoactivation of spindles in untreated (white squares), mRFP-CLASP2 wild-type overexpressing (black squares), and mRFP-CLASP2 S1234A mutant overexpressing (black circles) metaphase cells. Data points represent mean ± standard error from three independent experiments, n = 10 cells. (C) Calculated non-KT (top) and KT (bottom) MT half-life (min) in untreated, mRFP-CLASP2α overexpressing, and mRFP-CLASP2 S1234A mutant overexpressing U2OS cells. Error bars represent standard error from the regression analysis, *, $P < 0.001$, t test, n = 10 cells. (D) Examples of monopolar spindles from HeLa cells overexpressing GFP-CLASP2 wild-type treated with STLC, or overexpressing GFP-CLASP2 S1234A mutant. Cells were immunostained for acetylated tubulin, HURP, and PRC1 (all in red), and DNA counterstained with DAPI. (top) Merged images; (bottom) Grayscale images of the red marker. Bar, 5 μm. (E and F) Interquartile representation of median k-fiber or non-KT MT length in STLC-induced monopolar spindles overexpressing GFP-CLASP2 (wild type; n = 90) and monopoles overexpressing GFP-CLASP2 S1234A

Published October 8, 2012

non-KT–MT bundles that were acetylated and extensively decorated with PRC1, whereas HURP-labeled KT–MTs were shorter in monopolar spindles overexpressing GFP-CLASP2 S1234A, as indicated by the increased proximity between chromosomes and the center of the monopole (Fig. 8, D–F; and not depicted). Finally, we demonstrate that CLASP2 phosphorylation on S1234 and S1255 by Cdk1 and Plk1, respectively, increases with conditions that allow the establishment and stabilization of KT–MT attachments (Fig. 8 G). Overall, we conclude that CLASP2 phosphorylation on S1234, which enhances Plk1 recruitment to KTs while promoting additional CLASP2 phosphorylation by Plk1, defines a fine phospho-switch that stabilizes KT–MT attachments in human cells.

Discussion

In this study, we have identified Cdk1 and Plk1 as major kinases responsible for CLASP2 phosphorylation in mitosis. In particular, Cdk1-mediated phosphorylation of CLASP2 on S1234 at the C-terminal domain generates a Plk1-docking site important to recruit Plk1 to KTs and overall CLASP2 phosphorylation during mitosis. This molecular signature is conserved among clear CLASP2 orthologues in vertebrates, but is absent from CLASP1, indicating distinct functional regulation of CLASPs paralogues in vertebrates. Surprisingly, the same Plk1-binding motif is missing in the single CLASP orthologue reported in *X. tropicalis*, *D. melanogaster*, and *C. elegans*, suggesting that these might be functionally more closely related to mammalian CLASP1. However, we cannot exclude that other regions in these proteins fulfill the requirement to efficiently bind to and be phosphorylated by Plk1. Indeed, we observed that even CLASP2 is able to associate with Plk1 in vivo through its N-terminal domain. Moreover, although we did not observe a major band shift for CLASP1 in mitosis, several CLASP1-phosphorylated residues have been identified in large scale mass spectrometry studies of mitotic proteins and shown to be dependent on Plk1 activity (Kettenbach et al., 2011; Santamaria et al., 2011). In addition to Cdk1 and Plk1, we confirmed that GSK3β, directly or indirectly, plays a role in CLASP2 phosphorylation, which has recently been shown to regulate the association of CLASP2 with MT plus-ends during mitosis (Kumar et al., 2012).

CLASP1 was proposed to be part of a molecular switch at KTs that regulates KT–MT attachment stability through interaction with temporally distinct molecular partners (Manning et al., 2010). In this case, the transition to a higher stability condition was found to be promoted through an interaction with Astrin. Thus far, we have been unable to detect any phosphorylation-dependent differences in the in vivo binding capacity between CLASP2 and Astrin (Fig. S5). Alternatively, our present data indicates that CLASP2 phosphorylation on S1234 by Cdk1 stabilizes KT–MT attachments at least in part by mediating the recruitment of Plk1 to KTs, while promoting additional CLASP2 phosphorylation by Plk1. A similar Cdk1-mediated priming mechanism has been proposed for Plk1 recruitment to KTs by the SAC protein Bub1 (Qi et al., 2006), suggesting that multiple factors work in parallel to recruit Plk1 to KTs. Reduced Plk1 levels at KTs may have functional implications on other known Plk1 substrates at KTs involved in the temporal regulation of MT attachment stability, such as Kif2b (Hood et al., 2012), BubR1 (Lampson and Kapoor, 2005), CLIP-170 (Tanenbaum et al., 2006; Li et al., 2010), and Astrin (Manning et al., 2010; Kettenbach et al., 2011; Santamaria et al., 2011).

Incapacity to efficiently recruit Plk1 to KTs upon drug-mediated targeting of the PBD or overexpression of N-terminal deletion mutants was shown to cause chromosome alignment defects and mitotic arrest (Seong et al., 2002; Hanisch et al., 2006; Reindl et al., 2008; Watanabe et al., 2009). Here, we report that abolishment of a Plk1-binding motif or mutation of Plk1-mediated phosphorylation sites on the CLASP2 C terminal increases the incidence of chromosome alignment defects, suggesting that Cdk1- and Plk1-mediated CLASP2 phosphorylation regulates KT–MT attachments.

In addition to chromosome alignment defects, we found that overexpression of the nonphosphorylatable mutant of CLASP2 on S1234 leads to mitotic spindle collapse after bipolarization and formation of monopolar spindles. Plk1 kinase activity was previously implicated in the maintenance of spindle bipolarity (Sumara et al., 2004; Peters et al., 2006; Lénárt et al., 2007), but this role has been functionally dissociated from the correct PBD-mediated targeting of Plk1 to KTs (Seong et al., 2002; Hanisch et al., 2006). Thus, the spindle collapse into monopoles observed upon overexpression of CLASP2 S1234A mutant cannot solely be attributed to compromised Plk1 activity at KTs. Curiously, unstable KT–MTs and hyperstable non-KT–MTs resulting in spindle collapse after bipolarization have also been reported upon Plk1 kinase inhibition (Peters et al., 2006; Lénárt et al., 2007; Santamaria et al., 2007). This, together with our observation that the overexpression of wild-type CLASP2 hyperstabilizes non-KT–MTs, suggests that the formation of monopolar spindles upon overexpression of CLASP2 S1234A mutant results from unbalanced KT versus non-KT–MT stability (Kollu et al., 2009).

In this study, we found that CLASP2 is itself a Plk1 substrate. By means of a specific antibody developed against phosphorylated S1255, which is one of the four residues on the CLASP2 C terminal that was found to be directly phosphorylated by Plk1 in vitro (our study) and in vivo (Kettenbach et al., 2011), we found that CLASP2 is phosphorylated by Plk1 at KTs from prophase until telophase. Prophase phosphorylation is very high, yet total CLASP2 cannot easily be detected in KTs

mutant (n = 90). Lengths were measured between the central point of the monopole and the end of the respective MTs through the different z-sections. Medians are statistically different, $P < 0.0001$, Mann-Whitney t test. (G) Western blot of asynchronous, nocodazole-arrested, and nocodazole release into MG132 HeLa cell extracts. Total CLASP2 (left), S1234 (middle), and S1255 (right) phosphoepitopes were probed. Percentages indicate the fold increase relative to asynchronous cells normalized for α-tubulin.

Published October 8, 2012

at this stage. This possibly reflects the enrichment of a small phosphorylated form of CLASP2 at prophase KTs as a consequence of cyclin B import to the nucleus and an abrupt increase in Cdk1 activity at this stage (Hagting et al., 1999), which we show to be required for efficient Plk1-mediated phosphorylation of CLASP2 at KTs. Importantly, mutation of all four residues on the CLASP2 C terminal in a way that prevents their phosphorylation by Plk1 resulted in a significant delay in chromosome alignment, without affecting spindle bipolarity. This further suggests that CLASP2 phosphorylation on its C-terminal by Plk1 is functionally uncoupled from the role of CLASP2 in maintaining spindle bipolarity.

CLASP2 phosphorylation by Plk1 on S1255 was also strongly associated with centrosomes throughout mitosis. Taking into account that total CLASP2 is present at centrosomes throughout the cell cycle, we speculate that phosphorylation by Plk1 during mitosis may be related to CLASPs roles at centrosomes during spindle assembly (Samora et al., 2011; Logarinho et al., 2012). Indeed, mutation of CLASP2 C-terminal phosphorylation sites by Plk1 led to spindle orientation problems (unpublished data), and Plk1 kinase activity is required for spindle pole integrity (Oshimori et al., 2006; Lénárt et al., 2007).

Finally, small-molecule inhibitors specifically targeting the PBD of Plk1 have been recently shown to significantly suppress in vivo tumor growth by lowering the cell proliferation rate and triggering apoptosis (Yuan et al., 2011). Notably, overexpression of a CLASP2 phospho-mutant on its Plk1-binding motif dominates over the expression of endogenous CLASP2, leading to formation of monopolar spindles, chromosome alignment defects, and consequent cell death. As so, our findings open up the exciting possibility that administration of genetically modified Plk1 substrates (e.g., with nonphosphorylatable Plk1-binding motifs) might represent alternative therapeutic approaches in certain human cancers.

Materials and methods

Cell culture and drug treatments

Human HeLa, HeLa pEGFP-CLASP2α, HeLa H2B-mCherry (Schmitz et al., 2010), and U2OS PA-GFP-α-tubulin (Ganem et al., 2005) cells were grown in DME at 37°C in the presence of 5% CO_2 and supplemented with 10% FBS and antibiotics. To synchronize HeLa cell cultures in mitosis 5 µM of S-Trytil-L-Cysteine or 1.5 µM nocodazole were added to the media 16 h before harvesting by mitotic shake off. For kinase inhibitions, 5 µM of the proteasome inhibitor MG132 (EMD Millipore) was added to synchronized cells 1 h before drug treatment. For Cdk1 inhibition, we used 10 µM RO 3306 (Enzo Life Sciences), Plk1 was inhibited with 100 nM BI 2536 (Axon Medchem), GSK3β kinase activity was blocked by 40 mM LiCl, Mps1 was inhibited with 5 µM Mps1-IN-1 (Kwiatkowski et al., 2010), and Aurora B activity was inhibited with 2 µM ZM 447439 (AstraZeneca) according to the indicated times. For double thymidine block, HeLa cells were seeded at 30% confluence and treated for 18 h with 2 mM thymidine. After the first thymidine block, cells were washed and released for 9 h in DME + 10%FBS. After releasing, cells were blocked in 2mM thymidine for 17 h. After second block, cells were washed and released in DME + 10% FBS and collected at the indicated time points.

Constructs and transfections

To determine the specific localization of CLASP2, we used the previously described pEGFP-CLASP2α or mRFP-CLASP2α constructs (Akhmanova et al., 2001; Mimori-Kiyosue et al., 2005). pEGFP-CLASP2 S1234A was generated by site-directed mutagenesis with the following primers: forward, 5′-CAATGCCTACTCACTCCGCCCCACGCTCTCGAG-3′, and reverse, 5′-CTCGAGAGCGTGGGGCGGAGTGAGTAGGCATTG-3′. mRFP-CLASP2 S1234A was constructed by cutting pEGFP-CLASP2 S1234A with the enzyme BamHI and inserting it into the BamHI-digested mRFP-CLASP2α sequence. pEGFP-CLASP2 S1234D, S_A, and S_D Plk1 mutants were developed by inserting a synthesized sequence with the mutation in the pEGFP-CLASP2 construct. Transient and stable transfections into HeLa cells were performed using FuGENE HD (Roche) or Xtremegene HD (Roche). Human CLASP2 and CENP-E levels were reduced with specific small interfering RNA oligonucleotides (CLASP2, GACATACATGGGTCTTAGA; CENP-E, AAACACTTACTGCTCTCCAGTTT) as described previously (Harborth et al., 2001; Mimori-Kiyosue et al., 2005). For RNAi, cells were transfected 1 h after plating with Lipofectamine RNAiMAX-siRNA complexes according to the manufacturer's instructions (Invitrogen). Phenotypes were analyzed and quantified 72 h (for CLASP2) or 48 h (for CENP-E) after RNAi treatment, and protein depletion was monitored by Western blot.

Western blotting

Total protein HeLa cell extracts were separated on 9 or 7% acrylamide gels (ratio 80:1, acryl/bis), followed by Western blot with the antibodies: rat anti-CLASP2 1:100 (raised against a recombinant human CLASP2 fragment corresponding to nucleotides 90–876 from KIAA0627 cDNA; Maffini et al., 2009); rabbit anti-pS1234, anti-pS1255 1:500, and anti-CENP-E 1:500 (Santa Cruz Biotechnology, Inc.); mouse anti-Cyclin B1 1:1,500 (Cell Signaling Technology); and anti–α-tubulin 1:5000 (Sigma-Aldrich). HRP-conjugated secondary antibodies (GE Healthcare) were visualized with the ECL system (Thermo Fisher Scientific).

Immunofluorescence

HeLa cells were fixed in cold methanol or 4% paraformaldehyde, blocked with 10% FBS in PBS, and incubated with the following specified primary antibodies: rat anti-CLASP2 1:10 (Maffini et al., 2009); rabbit anti–CENP-E 1:300 (Santa Cruz Biotechnology, Inc.), anti-pS1255 1:500, anti-HURP 1:300 (Silljé et al., 2006) raised against a recombinant human HURP fragment from nucleotides 1–401 (gift from E. Nigg, Biozentrum, Basel, Switzerland), anti-PRC1 1:100 (Santa Cruz Biotechnology, Inc.), anti-GFP 1:1,000 raised against full-length recombinant protein; mouse anti-acetylated tubulin 1:2000 (Sigma-Aldrich); anti-Plk1 1:100 (Santa Cruz Biotechnology, Inc.); anti–α-tubulin 1:2,000 (Sigma-Aldrich); human anti-ACA 1:10,000 derived from autoimmune serum from Core Research for Evolutional Science and Technology patients (gift from W. Earnshaw, University of Edinburgh, Edinburgh, Scotland, UK). Cells were washed with PBS before and after incubation with Alexa Fluor secondary antibodies at a 1:1,000 dilution (Molecular Probes), and DNA was counterstained with 1 mg/ml DAPI (Maiato et al., 2003a). Chromosome spreads were performed by treating HeLa cells for 3 h with nocodazole, and then incubating them for 20 min in 75 mM KCl and processing them for immunofluorescence, as previously described (Maiato et al., 2003a). The antibodies against phosphorylated S1234 and S1255 in CLASP2 were generated in rabbits against the immunizing phosphorylated peptides 1227HSMPTHSSpPRSRDYNPY1243 and 1251PFNKSpALKEAMFDDD1265 (Abgent), respectively. Images were acquired with an AxioImager Z1 equipped with an AxioCam MR using immersion oil 63× 1.4 NA Plan-Apochromat objective, controlled by the AxioVision software (all from Carl Zeiss). Immunofluorescence images were deconvolved with AutoQuant software, and gamma intensity levels were adjusted with Adobe Photoshop. MT length was measured over z sections with Volocity software (Perkin-Elmer).

Fluorescence quantification

Protein accumulation at KTs of HeLa cells prepared for nocodazole treatment and immunostained with rat anti-CLASP2, rabbit anti-CENP-E, anti-pS1255, mouse anti-Plk1, and human anti-ACA was measured for individual KTs by quantification of the pixel gray levels of the focused z plane within a region of interest (ROI). Background was measured outside the ROI and subtracted from the measured fluorescence intensity inside the ROI. Results were normalized against a constitutive KT marker (ACA) with a custom routine written in MATLAB.

Image acquisition and time lapse microscopy

For time-lapse microscopy, cells were plated in 35 mm glass bottom microwell (14 mm, No 1.5 coverglass) dishes (MatTek Corporation), transfected and imaged in a heated environmental chamber (37°C). Four dimensional

datasets were acquired either with a Revolution spinning disc confocal system (Andor) based on an Olympus IX81 inverted microscope equipped with a Yokogawa CSU-22 spinning-disk confocal head (controlled by Andor-iQ software) or on a Nikon TE2000U inverted microscope equipped with a Yokogawa CSU-X1 spinning-disk confocal head (controlled by NIS-Elements software), both equipped with two laser lines (488 nm and 561 nm). 1.0-µm z stacks were collected every 2 or 3 min with a Plan-Apochromat 1.40 NA 60× immersion oil objective and images captured with an iXon^{EM} + Electron Multiplying CCD camera.

Photoactivation

For MT photoactivation, cells with metaphase plates were identified using differential interference contrast (DIC) microscopy. Spindle MTs were locally activated in one half spindle using a 500-ms pulse from a 405-nm (35%) laser (Photonic Instruments) on an Eclipse Ti microscope (Nikon) equipped with a spinning disk confocal attachment (Yokogawa). Fluorescence images were captured on a Hamamatsu ImageEM camera every 15 s for 6 min with a 100× oil-immersion 1.4 NA objective. DIC microscopy was then used to verify that cells did not enter anaphase throughout image acquisition. To quantify fluorescence dissipation after photoactivation, pixel intensities were measured within a 1-µm rectangular area surrounding the region of highest fluorescence intensity and background subtracted using an equal area from the nonactivated half spindle. The values were corrected for photobleaching by treating cells with 10 µM Taxol and determining the percentage of fluorescence loss during 6 min of image acquisition after photoactivation. Fluorescence values were normalized to the first time-point after photoactivation for each cell and the mean intensity at each time point was fit to a double exponential curve (A1 × exp[–k1t] + A2 × exp[–k2t]) using MatLab (Mathworks), where A1 represents the less stable non-KT–MT population and A2 the more stable KT–MT population with decay rates of k1 and k2, respectively. The turnover half-life for each process was calculated as ln2/k for each population of MTs.

Immunoprecipitation

Native protein extracts from asynchronously growing or mitotic shake-offs of HeLa, HeLa GFP-CLASP2 (wild-type), or HeLa GFP-CLASP2 S1234A cells were IP. 1 mg of total protein was incubated on IP buffer: 150 mM KCl, 75 mM Hepes, pH 7.5, 1.5 mM EGTA, 1.5 mM $MgCl_2$, 10% glycerol, 0.1% NP-40, protease, and phosphatase inhibitors. Protein extracts were incubated overnight with rotation at 4°C with the precipitating antibody (rabbit anti-GFP 1:100, mouse anti-Plk1 1:100, mouse and rabbit unspecific IgG 1:100), followed by the incubation with 40 µl of protein A magnetic beads for 1.5 h at 4°C. Unbound sample was recovered from the bead supernatant, and beads were washed with IP buffer. Precipitated proteins were eluted by boiling for 30 min in SDS sample buffer and analyzed by electrophoresis and Western blot with the appropriate antibody.

Identification of phosphorylation sites

To identify sites directly phosphorylated by Cdk1 and Plk1 in vitro, 1 µg recombinant human THE CLASP2 C terminal was incubated with 20 U of active Cdk1 (New England Biolabs) or Plk1 (EMD Millipore) for 1 h in the presence of 200 µM ATP. For radioactive kinase assays, reactions were performed with the addition of 10 µCi ATP-γP32. Phosphorylation sites within the CLASP2 C terminal were identified by mass spectrometry with an LTQ XL Ion trap mass spectrometer (Thermo Fisher Scientific) using MudPIT and SEQUEST software (http://fields.scripps.edu/sequest/) as previously described (Washburn et al., 2001).

Structural modeling

The 3D structure of the Plk1 PBD-MQSpTPL phosphopeptide complex [PDB entry 3P34, (Śledź et al., 2011)] was used as a model for the structural analysis of the interaction between the PBD and the 1222-THSpSPR-1227 Plk1-binding motif of CLASP2. Because no conformational changes occur in the PBD upon peptide binding (Cheng et al., 2003; Śledź et al., 2011), the MQSpTPL peptide sequence was mutated to the corresponding CLASP2 sequence with Coot (Emsley et al., 2010), the resulting complex was minimized with PHENIX (Adams et al., 2010), and the resulting 3D structure prepared with the PyMOL Molecular Graphics System, Version 1.5.0.1 Schrödinger, LLC.

Statistical analysis

All statistical analysis was performed with GraphPad Prism V5 (GraphPad Software, Inc.). Values were considered statistically different whenever $P < 0.05$.

Online supplemental material

In Fig. S1, the CLASP2 C terminal is characterized as the main phosphorylation cluster. Single kinase inhibitions were used to describe how Cdk1 and Plk1 contribute for CLASP2 mitotic shift. Furthermore, the evolutionary conservation of the identified phosphorylated residues is illustrated. CLASP2 phospho-antibodies are characterized in Fig. S2. Fig. S3 gives representative immunofluorescence images of mitotic HeLa cells transfected with GFP-CLASP2 S1234A and S1234D mutants. Similarly, the mitotic localization of S_A and S_D Plk1-CLASP2 mutants is described in Fig. S4. Fig. S5 shows a Western blot analysis from GFP-CLASP2 WT and S1234A immunoprecipitations, demonstrating that CLASP2 phosphorylation on S1234 is not required for CLASP2-Astrin interaction. Tables S1 and S2 summarize the phospho-peptides identified by mass spectrometry analysis of the CLASP2 C terminal after in vitro phosphorylation by Cdk1 (Table S1) and Plk1 (Table S2). Video S1 illustrates an HeLa cell transiently transfected with GFP-CLASP2 S1234A undergoing mitotic spindle collapse. Video S2 shows cell death of an HeLa cell as a consequence of GFP-CLASP2 S1234A overexpression. Video S3 depicts a HeLa cell transiently expressing GFP-CLASP2 (wild type). Video S4 demonstrates how GFP-CLASP2 S1234A mutant expression impairs normal mitotic timing and fidelity. Video S5 shows how CLASP2 S_A Plk1 mutant expression compromises normal mitotic timing and chromosome alignment. Online supplemental material is available at http://www.jcb.org/cgi/content/full/jcb.201203091/DC1.

We would like to thank all colleagues that provided invaluable reagents.

We would like to thank Fundação para a Ciência e a Tecnologia (FCT) of Portugal for fellowships SFRH/BD/32976/2006 (to A.R.R. Maia), SFRH/BPD/79229/2011 (to Z. Garcia) and SFRH/BPD/26780/2006 (to S. Maffini). We acknowledge financial support from National Institutes of Health (NIH)/National Institute of General Medical Sciences grant GM088313 (to I.M. Cheeseman), NIH grant 5R01-GM078373 and American Heart Association grant-in-aid 10GRNT4230026 (to I. Kaverina), NIH grant GM51542 (to D.A. Compton), and FCT grant REEQ/564/BIO/2005 (EU-FEDER and POCI 2010, to S. Macedo-Ribeiro). Work in the laboratory of H. Maiato is funded by grants PTDC/SAU-GMG/099704/2008 and PTDC/SAU-ONC/112917/2009 from FCT (COMPETE-FEDER), the Human Frontier Research Program (with I.C.), and the seventh framework program grant PRECISE from the European Research Council.

H. Maiato and A.R.R. Maia declare that a patent application protecting the commercial use of CLASP2 phosphorylation mutants is currently being filed.

Submitted: 19 March 2012
Accepted: 17 September 2012

References

Adams, P.D., P.V. Afonine, G. Bunkóczi, V.B. Chen, I.W. Davis, N. Echols, J.J. Headd, L.W. Hung, G.J. Kapral, R.W. Grosse-Kunstleve, et al. 2010. PHENIX: a comprehensive Python-based system for macromolecular structure solution. *Acta Crystallogr. D Biol. Crystallogr.* 66:213–221. http://dx.doi.org/10.1107/S0907444909052925

Akhmanova, A., C.C. Hoogenraad, K. Drabek, T. Stepanova, B. Dortland, T. Verkerk, W. Vermeulen, B.M. Burgering, C.I. De Zeeuw, F. Grosveld, and N. Galjart. 2001. Clasps are CLIP-115 and -170 associating proteins involved in the regional regulation of microtubule dynamics in motile fibroblasts. *Cell.* 104:923–935. http://dx.doi.org/10.1016/S0092-8674(01)00288-4

Bader, J.R., J.M. Kasuboski, M. Winding, P.S. Vaughan, E.H. Hinchcliffe, and K.T. Vaughan. 2011. Polo-like kinase1 is required for recruitment of dynein to kinetochores during mitosis. *J. Biol. Chem.* 286:20769–20777. http://dx.doi.org/10.1074/jbc.M111.226605

Bakhoum, S.F., and D.A. Compton. 2011. Kinetochores and disease: keeping microtubule dynamics in check! *Curr. Opin. Cell Biol.* 24:64–70.

Bakhoum, S.F., G. Genovese, and D.A. Compton. 2009a. Deviant kinetochore microtubule dynamics underlie chromosomal instability. *Curr. Biol.* 19:1937–1942. http://dx.doi.org/10.1016/j.cub.2009.09.055

Bakhoum, S.F., S.L. Thompson, A.L. Manning, and D.A. Compton. 2009b. Genome stability is ensured by temporal control of kinetochore-microtubule dynamics. *Nat. Cell Biol.* 11:27–35. http://dx.doi.org/10.1038/ncb1809

Cheng, K.Y., E.D. Lowe, J. Sinclair, E.A. Nigg, and L.N. Johnson. 2003. The crystal structure of the human polo-like kinase-1 polo box domain and its phospho-peptide complex. *EMBO J.* 22:5757–5768. http://dx.doi.org/10.1093/emboj/cdg558

Ditchfield, C., V.L. Johnson, A. Tighe, R. Ellston, C. Haworth, T. Johnson, A. Mortlock, N. Keen, and S.S. Taylor. 2003. Aurora B couples chromosome alignment with anaphase by targeting BubR1, Mad2, and Cenp-E to kinetochores. *J. Cell Biol.* 161:267–280. http://dx.doi.org/10.1083/jcb.200208091

Efimov, A., A. Kharitonov, N. Efimova, J. Loncarek, P.M. Miller, N. Andreyeva, P. Gleeson, N. Galjart, A.R. Maia, I.X. McLeod, et al. 2007. Asymmetric CLASP-dependent nucleation of noncentrosomal microtubules at the trans-Golgi network. *Dev. Cell*. 12:917–930. http://dx.doi.org/10.1016/j.devcel.2007.04.002

Elia, A.E., L.C. Cantley, and M.B. Yaffe. 2003a. Proteomic screen finds pSer/pThr-binding domain localizing Plk1 to mitotic substrates. *Science*. 299:1228–1231. http://dx.doi.org/10.1126/science.1079079

Elia, A.E., P. Rellos, L.F. Haire, J.W. Chao, F.J. Ivins, K. Hoepker, D. Mohammad, L.C. Cantley, S.J. Smerdon, and M.B. Yaffe. 2003b. The molecular basis for phosphodependent substrate targeting and regulation of Plks by the Polo-box domain. *Cell*. 115:83–95. http://dx.doi.org/10.1016/S0092-8674(03)00725-6

Emsley, P., B. Lohkamp, W.G. Scott, and K. Cowtan. 2010. Features and development of Coot. *Acta Crystallogr. D Biol. Crystallogr.* 66:486–501. http://dx.doi.org/10.1107/S0907444910007493

Ganem, N.J., K. Upton, and D.A. Compton. 2005. Efficient mitosis in human cells lacking poleward microtubule flux. *Curr. Biol.* 15:1827–1832. http://dx.doi.org/10.1016/j.cub.2005.08.065

Hagting, A., M. Jackman, K. Simpson, and J. Pines. 1999. Translocation of cyclin B1 to the nucleus at prophase requires a phosphorylation-dependent nuclear import signal. *Curr. Biol.* 9:680–689. http://dx.doi.org/10.1016/S0960-9822(99)80308-X

Hanisch, A., A. Wehner, E.A. Nigg, and H.H. Silljé. 2006. Different Plk1 functions show distinct dependencies on Polo-Box domain-mediated targeting. *Mol. Biol. Cell*. 17:448–459. http://dx.doi.org/10.1091/mbc.E05-08-0801

Harborth, J., S.M. Elbashir, K. Bechert, T. Tuschl, and K. Weber. 2001. Identification of essential genes in cultured mammalian cells using small interfering RNAs. *J. Cell Sci.* 114:4557–4565.

Hegemann, B., J.R. Hutchins, O. Hudecz, M. Novatchkova, J. Rameseder, M.M. Sykora, S. Liu, M. Mazanek, P. Lénárt, J.K. Hériché, et al. 2011. Systematic phosphorylation analysis of human mitotic protein complexes. *Sci. Signal.* 4:rs12. http://dx.doi.org/10.1126/scisignal.2001993

Hood, E.A., A.N. Kettenbach, S.A. Gerber, and D.A. Compton. 2012. Plk1 regulates the kinesin-13 protein Kif2b to promote faithful chromosome segregation. *Mol. Biol. Cell*. 23:2264–2274. http://dx.doi.org/10.1091/mbc.E11-12-1013

Kang, Y.H., J.E. Park, L.R. Yu, N.K. Soung, S.M. Yun, J.K. Bang, Y.S. Seong, H. Yu, S. Garfield, T.D. Veenstra, and K.S. Lee. 2006. Self-regulated Plk1 recruitment to kinetochores by the Plk1-PBIP1 interaction is critical for proper chromosome segregation. *Mol. Cell*. 24:409–422. http://dx.doi.org/10.1016/j.molcel.2006.10.016

Kettenbach, A.N., D.K. Schweppe, B.K. Faherty, D. Pechenick, A.A. Pletnev, and S.A. Gerber. 2011. Quantitative phosphoproteomics identifies substrates and functional modules of Aurora and Polo-like kinase activities in mitotic cells. *Sci. Signal.* 4:rs5. http://dx.doi.org/10.1126/scisignal.2001497

Kirschner, M., and T. Mitchison. 1986. Beyond self-assembly: from microtubules to morphogenesis. *Cell*. 45:329–342. http://dx.doi.org/10.1016/0092-8674(86)90318-1

Kollu, S., S.F. Bakhoum, and D.A. Compton. 2009. Interplay of microtubule dynamics and sliding during bipolar spindle formation in mammalian cells. *Curr. Biol.* 19:2108–2113. http://dx.doi.org/10.1016/j.cub.2009.10.056

Kumar, P., K.S. Lyle, S. Gierke, A. Matov, G. Danuser, and T. Wittmann. 2009. GSK3beta phosphorylation modulates CLASP-microtubule association and lamella microtubule attachment. *J. Cell Biol.* 184:895–908. http://dx.doi.org/10.1083/jcb.200901042

Kumar, P., M.S. Chimenti, H. Pemble, A. Schönichen, O. Thompson, M.P. Jacobson, and T. Wittmann. 2012. Multisite phosphorylation disrupts arginine-glutamate salt bridge networks required for binding of cytoplasmic linker-associated protein 2 (CLASP2) to end-binding protein 1 (EB1). *J. Biol. Chem.* 287:17050–17064.

Kwiatkowski, N., N. Jelluma, P. Filippakopoulos, M. Soundararajan, M.S. Manak, M. Kwon, H.G. Choi, T. Sim, Q.L. Deveraux, S. Rottmann, et al. 2010. Small-molecule kinase inhibitors provide insight into Mps1 cell cycle function. *Nat. Chem. Biol.* 6:359–368. http://dx.doi.org/10.1038/nchembio.345

Lampson, M.A., and T.M. Kapoor. 2005. The human mitotic checkpoint protein BubR1 regulates chromosome-spindle attachments. *Nat. Cell Biol.* 7:93–98. http://dx.doi.org/10.1038/ncb1208

Lénárt, P., M. Petronczki, M. Steegmaier, B. Di Fiore, J.J. Lipp, M. Hoffmann, W.J. Rettig, N. Kraut, and J.M. Peters. 2007. The small-molecule inhibitor BI 2536 reveals novel insights into mitotic roles of polo-like kinase 1. *Curr. Biol.* 17:304–315. http://dx.doi.org/10.1016/j.cub.2006.12.046

Li, H., X.S. Liu, X. Yang, Y. Wang, Y. Wang, J.R. Turner, and X. Liu. 2010. Phosphorylation of CLIP-170 by Plk1 and CK2 promotes timely formation of kinetochore-microtubule attachments. *EMBO J.* 29:2953–2965. http://dx.doi.org/10.1038/emboj.2010.174

Liu, J., Z. Wang, K. Jiang, L. Zhang, L. Zhao, S. Hua, F. Yan, Y. Yang, D. Wang, C. Fu, et al. 2009. PRC1 cooperates with CLASP1 to organize central spindle plasticity in mitosis. *J. Biol. Chem.* 284:23059–23071. http://dx.doi.org/10.1074/jbc.M109.009670

Logarinho, E., S. Maffini, M. Barisic, A. Marques, A. Toso, P. Meraldi, and H. Maiato. 2012. CLASPs prevent irreversible multipolarity by ensuring spindle-pole resistance to traction forces during chromosome alignment. *Nat. Cell Biol.* 14:295–303

Maffini, S., A.R. Maia, A.L. Manning, Z. Maliga, A.L. Pereira, M. Junqueira, A. Shevchenko, A. Hyman, J.R. Yates III, N. Galjart, et al. 2009. Motor-independent targeting of CLASPs to kinetochores by CENP-E promotes microtubule turnover and poleward flux. *Curr. Biol.* 19:1566–1572. http://dx.doi.org/10.1016/j.cub.2009.07.059

Maiato, H., E.A. Fairley, C.L. Rieder, J.R. Swedlow, C.E. Sunkel, and W.C. Earnshaw. 2003a. Human CLASP1 is an outer kinetochore component that regulates spindle microtubule dynamics. *Cell*. 113:891–904. http://dx.doi.org/10.1016/S0092-8674(03)00465-3

Maiato, H., C.L. Rieder, W.C. Earnshaw, and C.E. Sunkel. 2003b. How do kinetochores CLASP dynamic microtubules? *Cell Cycle*. 2:511–514. http://dx.doi.org/10.4161/cc.2.6.576

Manning, A.L., N.J. Ganem, S.F. Bakhoum, M. Wagenbach, L. Wordeman, and D.A. Compton. 2007. The kinesin-13 proteins Kif2a, Kif2b, and Kif2c/MCAK have distinct roles during mitosis in human cells. *Mol. Biol. Cell*. 18:2970–2979. http://dx.doi.org/10.1091/mbc.E07-02-0110

Manning, A.L., S.F. Bakhoum, S. Maffini, C. Correia-Melo, H. Maiato, and D.A. Compton. 2010. CLASP1, astrin and Kif2b form a molecular switch that regulates kinetochore-microtubule dynamics to promote mitotic progression and fidelity. *EMBO J.* 29:3531–3543. http://dx.doi.org/10.1038/emboj.2010.230

Matos, I., and H. Maiato. 2011. Prevention and correction mechanisms behind anaphase synchrony: implications for the genesis of aneuploidy. *Cytogenet. Genome Res.* 133:243–253. http://dx.doi.org/10.1159/000323803

Mimori-Kiyosue, Y., I. Grigoriev, G. Lansbergen, H. Sasaki, C. Matsui, F. Severin, N. Galjart, F. Grosveld, I. Vorobjev, S. Tsukita, and A. Akhmanova. 2005. CLASP1 and CLASP2 bind to EB1 and regulate microtubule plus-end dynamics at the cell cortex. *J. Cell Biol.* 168:141–153. http://dx.doi.org/10.1083/jcb.200405094

Mollinari, C., J.P. Kleman, W. Jiang, G. Schoehn, T. Hunter, and R.L. Margolis. 2002. PRC1 is a microtubule binding and bundling protein essential to maintain the mitotic spindle midzone. *J. Cell Biol.* 157:1175–1186. http://dx.doi.org/10.1083/jcb.200111052

Nishino, M., Y. Kurasawa, R. Evans, S.H. Lin, B.R. Brinkley, and L.Y. Yu-Lee. 2006. NudC is required for Plk1 targeting to the kinetochore and chromosome congression. *Curr. Biol.* 16:1414–1421. http://dx.doi.org/10.1016/j.cub.2006.05.052

Oshimori, N., M. Ohsugi, and T. Yamamoto. 2006. The Plk1 target Kizuna stabilizes mitotic centrosomes to ensure spindle bipolarity. *Nat. Cell Biol.* 8:1095–1101. http://dx.doi.org/10.1038/ncb1474

Pereira, A.L., A.J. Pereira, A.R. Maia, K. Drabek, C.L. Sayas, P.J. Hergert, M. Lince-Faria, I. Matos, C. Duque, T. Stepanova, et al. 2006. Mammalian CLASP1 and CLASP2 cooperate to ensure mitotic fidelity by regulating spindle and kinetochore function. *Mol. Biol. Cell*. 17:4526–4542. http://dx.doi.org/10.1091/mbc.E06-07-0579

Peters, U., J. Cherian, J.H. Kim, B.H. Kwok, and T.M. Kapoor. 2006. Probing cell-division phenotype space and Polo-like kinase function using small molecules. *Nat. Chem. Biol.* 2:618–626. http://dx.doi.org/10.1038/nchembio826

Piperno, G., M. LeDizet, and X.J. Chang. 1987. Microtubules containing acetylated alpha-tubulin in mammalian cells in culture. *J. Cell Biol.* 104:289–302. http://dx.doi.org/10.1083/jcb.104.2.289

Qi, W., Z. Tang, and H. Yu. 2006. Phosphorylation- and polo-box-dependent binding of Plk1 to Bub1 is required for the kinetochore localization of Plk1. *Mol. Biol. Cell*. 17:3705–3716. http://dx.doi.org/10.1091/mbc.E06-03-0240

Reindl, W., J. Yuan, A. Krämer, K. Strebhardt, and T. Berg. 2008. Inhibition of polo-like kinase 1 by blocking polo-box domain-dependent protein-protein interactions. *Chem. Biol.* 15:459–466. http://dx.doi.org/10.1016/j.chembiol.2008.03.013

Samora, C.P., B. Mogessie, L. Conway, J.L. Ross, A. Straube, and A.D. McAinsh. 2011. MAP4 and CLASP1 operate as a safety mechanism to

maintain a stable spindle position in mitosis. *Nat. Cell Biol.* 13:1040–1050. http://dx.doi.org/10.1038/ncb2297

Santamaria, A., R. Neef, U. Eberspächer, K. Eis, M. Husemann, D. Mumberg, S. Prechtl, V. Schulze, G. Siemeister, L. Wortmann, et al. 2007. Use of the novel Plk1 inhibitor ZK-thiazolidinone to elucidate functions of Plk1 in early and late stages of mitosis. *Mol. Biol. Cell*. 18:4024–4036. http://dx.doi.org/10.1091/mbc.E07-05-0517

Santamaria, A., B. Wang, S. Elowe, R. Malik, F. Zhang, M. Bauer, A. Schmidt, H.H. Sillje, R. Korner, and E.A. Nigg. 2011. The Plk1-dependent phosphoproteome of the early mitotic spindle. *Mol. Cell. Proteomics*. 10:M110.004457.

Schmitz, M.H., M. Held, V. Janssens, J.R. Hutchins, O. Hudecz, E. Ivanova, J. Goris, L. Trinkle-Mulcahy, A.I. Lamond, I. Poser, et al. 2010. Live-cell imaging RNAi screen identifies PP2A-B55alpha and importin-beta1 as key mitotic exit regulators in human cells. *Nat. Cell Biol.* 12:886–893. http://dx.doi.org/10.1038/ncb2092

Seong, Y.S., K. Kamijo, J.S. Lee, E. Fernandez, R. Kuriyama, T. Miki, and K.S. Lee. 2002. A spindle checkpoint arrest and a cytokinesis failure by the dominant-negative polo-box domain of Plk1 in U-2 OS cells. *J. Biol. Chem.* 277:32282–32293. http://dx.doi.org/10.1074/jbc.M202602200

Silljé, H.H., S. Nagel, R. Körner, and E.A. Nigg. 2006. HURP is a Ran-importin beta-regulated protein that stabilizes kinetochore microtubules in the vicinity of chromosomes. *Curr. Biol.* 16:731–742. http://dx.doi.org/10.1016/j.cub.2006.02.070

Śledź, P., C.J. Stubbs, S. Lang, Y.Q. Yang, G.J. McKenzie, A.R. Venkitaraman, M. Hyvönen, and C. Abell. 2011. From crystal packing to molecular recognition: prediction and discovery of a binding site on the surface of polo-like kinase 1. *Angew. Chem. Int. Ed. Engl.* 50:4003–4006. http://dx.doi.org/10.1002/anie.201008019

Sumara, I., J.F. Giménez-Abián, D. Gerlich, T. Hirota, C. Kraft, C. de la Torre, J. Ellenberg, and J.M. Peters. 2004. Roles of polo-like kinase 1 in the assembly of functional mitotic spindles. *Curr. Biol.* 14:1712–1722. http://dx.doi.org/10.1016/j.cub.2004.09.049

Tanenbaum, M.E., N. Galjart, M.A. van Vugt, and R.H. Medema. 2006. CLIP-170 facilitates the formation of kinetochore-microtubule attachments. *EMBO J.* 25:45–57. http://dx.doi.org/10.1038/sj.emboj.7600916

Vassilev, L.T., C. Tovar, S. Chen, D. Knezevic, X. Zhao, H. Sun, D.C. Heimbrook, and L. Chen. 2006. Selective small-molecule inhibitor reveals critical mitotic functions of human CDK1. *Proc. Natl. Acad. Sci. USA*. 103:10660–10665. http://dx.doi.org/10.1073/pnas.0600447103

Washburn, M.P., D. Wolters, and J.R. Yates III. 2001. Large-scale analysis of the yeast proteome by multidimensional protein identification technology. *Nat. Biotechnol.* 19:242–247. http://dx.doi.org/10.1038/85686

Watanabe, N., T. Sekine, M. Takagi, J. Iwasaki, N. Imamoto, H. Kawasaki, and H. Osada. 2009. Deficiency in chromosome congression by the inhibition of Plk1 polo box domain-dependent recognition. *J. Biol. Chem.* 284:2344–2353. http://dx.doi.org/10.1074/jbc.M805308200

Yuan, J., M. Sanhaji, A. Krämer, W. Reindl, M. Hofmann, N.N. Kreis, B. Zimmer, T. Berg, and K. Strebhardt. 2011. Polo-box domain inhibitor poloxin activates the spindle assembly checkpoint and inhibits tumor growth in vivo. *Am. J. Pathol.* 179:2091–2099. http://dx.doi.org/10.1016/j.ajpath.2011.06.031

Zhai, Y., P.J. Kronebusch, and G.G. Borisy. 1995. Kinetochore microtubule dynamics and the metaphase-anaphase transition. *J. Cell Biol.* 131:721–734. http://dx.doi.org/10.1083/jcb.131.3.721